

A Survey on Generative Diffusion Model

Hanqun Cao, Cheng Tan, Zhangyang Gao, Guangyong Chen, Pheng-Ann Heng, *Senior Member, IEEE*, and Stan Z. Li, *Fellow, IEEE*

Abstract—Deep learning shows excellent potential in generation tasks thanks to deep latent representation. Generative models are classes of models that can generate observations randomly with respect to certain implied parameters. Recently, the diffusion Model has become a rising class of generative models by virtue of its power-generating ability. Nowadays, great achievements have been reached. More applications except for computer vision, speech generation, bioinformatics, and natural language processing are to be explored in this field. However, the diffusion model has its genuine drawback of a slow generation process, single data types, low likelihood, and the inability for dimension reduction. They are leading to many enhanced works. This survey makes a summary of the field of the diffusion model. We first state the main problem with two landmark works – DDPM and DSM, and a unified landmark work – Score SDE. Then, we present classified improved techniques for existing problems in the diffusion-based model field. For model speed-up improvement, we present a diverse range of advanced techniques to speed up the diffusion models – training schedule, training-free sampling, mixed-modeling, and score & diffusion unification. For data structure diversification, we present improved techniques for applying diffusion models in continuous space, discrete space, and constraint space. For likelihood optimization, we present theoretical methods for improving ELBO and minimizing the variational gap. For dimension reduction, we present several techniques to solve the high dimension problem. Regarding existing models, we also provide a benchmark of FID score, IS, and NLL according to specific NFE. Moreover, applications with diffusion models are introduced including computer vision, sequence modeling, audio, and AI for science. Finally, there is a summarization of this field together with limitations & further directions. Summation of existing well-classified methods is in our Github: <https://github.com/chq1155/A-Survey-on-Generative-Diffusion-Model>.

Index Terms—Diffusion Model, advanced improvement on diffusion, diffusion application.

1 INTRODUCTION

How can we empower machines with human-like imagination? Deep generative models, e.g., VAE [1], [2], [3], [4], EBM [5], [6], [7], [8], GAN [9], [10], [11], [12], [13], normalizing flow [14], [15], [16], [17], [18], [19] and diffusion models [20], [21], [22], [23], [24], have shown great potential in creating new patterns that humans cannot properly distinguish. We focus on diffusion-based generative models, which do not require aligning posterior distributions as VAE, dealing with intractable partition functions as EBM, training additional discriminators as GAN, or imposing network constraints as normalizing flow. Thanks to the aforementioned virtues, diffusion-based methods have drawn considerable attention from computer vision, and natural language processing to graph analysis. However, there is still a lack of systematic taxonomy and analysis of research progress on diffusion models.

Advances in the diffusion model have provided tractable probabilistic parameterization for describing the model, a

stable training procedure with sufficient theoretical support, and a unified loss function design with high simplicity. The diffusion model aims to transform the prior data distribution into random noise before revising the transformations step by step to rebuild a brand new sample with the same distribution as the prior [25]. In recent years, the diffusion model has displayed its exquisite potential in the field of computer vision (CV) [?], [20], [26], [27], [28], [29], [30], [31], [32], [33], [34], [35], [36], [37], sequence modeling [38], [39], [40], [41], audio processing [42], [43], [44], [45], [46], [47], [48], [49], [50], [51], and AI for science [52], [53], [54], [55], [56]. Inspired by the so-far successes of the diffusion model in these popular domains, applying diffusion models to generation-related tasks of the other domains would be a favorable path for exploiting powerful generative capacity.

On the other hand, the diffusion model has the inherent drawback of plenty of sampling steps and a long sampling time compared to Generative Adversarial Networks (GANs) and Variational Auto-Encoders (VAEs). Since diffusion models leverage a Markov process to convert data distribution via tiny perturbations, a large number of diffusion steps are required in both the training and inference phases. Thus, it takes more time to sample from a random noise until it eventually alters to high-quality data similar to the prior. Furthermore, other problems such as likelihood optimization and the inability of dimension reduction also count. Therefore, lots of works aspired to accelerate the diffusion process along with improving sampling quality [60], [61], [62]. For example, DPM-solver takes the advantage of ODE’s stability to generate samples of the State-of-the-art within 10 steps [63]. D3PM [64] not only proposes hybrid training loss but also text & categorical data. We summarize im-

- H. Cao is with the Department of Math, The Chinese University of Hong Kong, Hong Kong, China, and also with the AI Lab, School of Engineering, Westlake University, Hangzhou, China, and Zhejiang Lab, Hangzhou, China. Email: 1155141481@link.cuhk.edu.hk.
- C. Tan and Z. Gao are with Zhejiang University, Hangzhou, China, and also with the AI Lab, School of Engineering, Westlake University, Hangzhou, China. Email: tancheng, gaozhangyang@westlake.edu.cn.
- G. Chen is with Zhejiang Lab, Hangzhou, China. Email: gychen@zhejianglab.com.
- P.-A. Heng is with the Department of Computer Science and Engineering, The Chinese University of Hong Kong, Hong Kong, China.
- Stan Z. Li is with the AI Lab, School of Engineering, Westlake University, Hangzhou, China. Email: Stan.ZQ.Li@westlake.edu.cn.
- H. Cao, C. Tan, and Z. Gao contributed equally to this work.

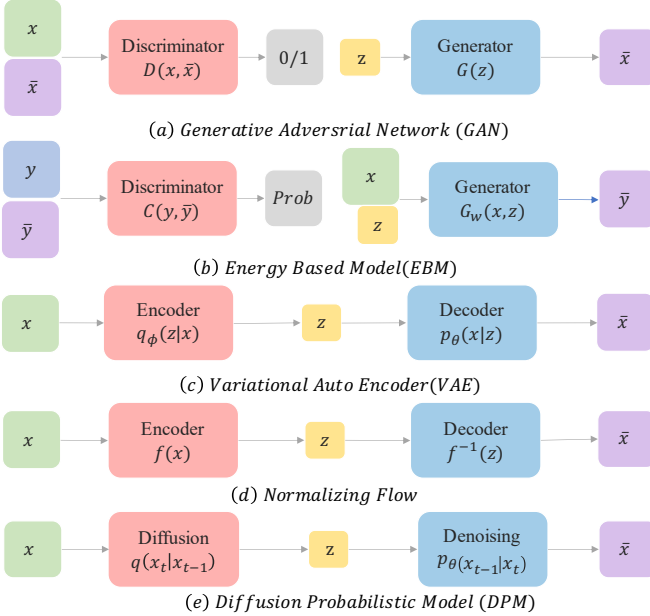


Fig. 1. Generative Models Pipeline. **(a)** Generative Adversarial Net (GAN) [57] applies adversarial training strategy onto the generator to generate lifelike samples like input distributions. **(b)** Energy-Based Model (EBM) [58] designs a suitable energy function for pair-wise energy matching between conditions and samples, similar to a generative discriminator in GAN. **(c)** Variational Auto-Encoder (VAE) [59] applies the encoder to project the prior into a latent space with reduced dimension from which the decoder can sample. **(d)** Normalizing flow (NF) [18] employs a well-designed reversible flow function for turning input into latent variable before returning to samples with the inverse of flow function. **(e)** Diffusion model gradually injects noise into original data until it turns to the known noise distribution before reversing each step in the sampling steps.

provement works on diffusion models into four classes. (1) Speed-up improvement, (2) Data structure diversification, (3) Likelihood optimization, and (4) Dimension reduction. The detailed contents are provided in Section 3.

Hence, based on the wide range of applications along with multi-perspective thinking on algorithm improvement, we target to provide a detailed survey about current aspects of diffusion models. By classifying enhanced algorithms and applications in other domains, the core contributions of this review are as follows:

- Summarize essence mathematical formulation and derivation of fundamental algorithms in the field of diffusion model, including taking advantage of training strategy, and sampling algorithm.
- Present comprehensive and up-to-date classification of improved diffusion algorithms and divide them into four proposals, which are speed-up improvement, structure diversification, likelihood optimization, and dimension reduction.
- Provide extensive statements about the application of diffusion models on computer vision, natural language processing, bioinformatics, and speech processing which include domain-specialized problem formulation, related datasets, evaluation metrics, and downstream tasks, along with sets of benchmarks.
- Clarify current limitations of models and possible further-proof directions concerning the field of dif-

fusion models.

2 PROBLEM STATEMENT

2.1 Notions and Definitions

2.1.1 State

States are a set of data distributions that describe the whole process of diffusion models. In the beginning, the noise is gradually injected into the starting distribution, which is called starting state x_0 . With enough steps of noise injection, the distribution finally comes into a known noise distribution (mostly Gaussian), which is called the prior state x_T (Discrete)/ x_1 (Continuous). Then, the other distributions between the starting state and the prior state are called intermediate states x_t .

2.1.2 Process & Transition Kernel

As mentioned above, the process that transforms the starting state into the tractable noise is the forward/diffusion process F . The process following the opposite direction to the forward process is called reverse/denoised process R . The reverse process samples the noise gradients step by step into the samples as the starting state. In either process, the interchange between any two states is achieved by the transition kernel. The most frequently used kernel is the Markov kernel since it ensures randomness and tractability in the forward process and the reverse process.

Forward Process & Kernel: To present a unified framework, the forward process consists of plenty of forward steps which are the forward transition kernels:

$$F(x, \sigma) = F_T(x_{T-1}, \sigma_T) \circ \dots \circ F_t(x_{t-1}, \sigma_t) \circ \dots \circ F_1(x_0, \sigma_1) \quad (1)$$

$$x_t = F_t(x_{t-1}, \sigma_t) \quad (2)$$

Different from the discrete case, for any time $0 \leq t < s \leq 1$, the forward process is defined:

$$F(x, \sigma) = F_{s1}(x_s, \sigma_{s1}) \circ F_{ts}(x_t, \sigma_{ts}) \circ F_{0t}(x_0, \sigma_{0t}) \quad (3)$$

$$x_s = F_{ts}(x_s, \sigma_{ts}) \quad (4)$$

where F_t is the forward transition kernel at time t with the variables intermediate state x_{t-1} & x_{ts} and the noise scale σ_t & σ_{ts} . The difference between this expression and normalizing flow is the variable noise scale, which controls the randomness of the whole process. When the noise is close to 0, the process will become the normalizing flow which is deterministic.

Reverse Process & Kernels: Similarly, the reverse process is defined as:

$$R(x, \sigma) = R_1(x_1, \sigma_1) \circ \dots \circ R_t(x_t, \sigma_t) \circ \dots \circ R_T(x_T, \sigma_T) \quad (5)$$

$$x_{t-1} = R_t(x_t, \sigma_t) \quad (\text{Discrete}) \quad (6)$$

$$R(x, \sigma) = R_{t0}(x_t, \sigma_{t0}) \circ \dots \circ R_{st}(x_s, \sigma_{st}) \circ \dots \circ R_{1s}(x_T, \sigma_{1s}) \quad (7)$$

$$x_t = R_{st}(x_s, \sigma_{st}) \quad (\text{Continuous}) \quad (8)$$

where R_t is the reverse transition kernel at time t with the variables intermediate state x_t & x_{st} and the noise scale σ_t & σ_{st} .

Usually, the reverse process in practice is implemented by the sampling process, which gradually collects the reverse gradients and reconstructs the samples.

Pipeline: Denote the sampled data as \tilde{x}_0 the generalized process can be expressed as:

$$\tilde{x}_0 = [R_1(x_1, \sigma_1) \cdots \circ R_t(x_t, \sigma_t) \cdots \circ R_T(x_T, \sigma_T)] \circ [F_T(x_{T-1}, \sigma_T) \cdots \circ F_t(x_{t-1}, \sigma_t) \cdots \circ F_1(x_0, \sigma_1)] \quad (9)$$

$$\tilde{x}_0 = [R_{t0}(x_t, \sigma_{t0}) \cdots \circ R_{st}(x_s, \sigma_{st}) \cdots \circ R_{1s}(x_T, \sigma_{1s})] \circ [F_{s1}(x_s, \sigma_{s1})F_{0t} \circ F_{ts}(x_t, \sigma_{ts}) \circ F_{0t}(x_0, \sigma_{0t})] \quad (10)$$

2.1.3 Discrete and continuous

Taking the perturbation kernel to sufficiently small, the whole discrete process will contain infinite steps. To tackle the mechanism behind this situation, the continuous process starting from time 0 and ending at time 1 is used in many improved algorithms [65], [66] to obtain better performance. Compared to a discrete process, the continuous one enables the extraction of any information from any time state. Further, assuming the change of perturbation kernel is slight enough, the continuous process enjoys better theoretical support.

2.1.4 Training Objective

The diffusion model as one type of the generative model follows the same training objective as variational autoregressive-encoder and normalizing flow, which is keeping starting distribution x_0 and sample distribution \tilde{x}_0 as close as possible. This is implemented by maximizing the log-likelihood [25]:

$$\mathbb{E}_{F(x_0, \sigma)} [-\log R(x_T, \tilde{\sigma})] \quad (11)$$

where the $\tilde{\sigma}$ in the reverse process differs from the one in the forward process.

2.2 Problem Formulation

Based on the unified framework, two discrete landmark works – DDPM [67] and Denoising Score Matching (DSM) [68], along with the unified continuous landmark works – Score SDE are stated below with customized transition kernels and training objectives.

2.2.1 Diffusion Model Formulation

The original idea of the diffusion probabilistic model is to recreate a specific distribution that starts with random noise. Thus, the distributions of generated samples are required to be as close as the ones of the original samples.

DDPM Forward Process: Based on the unified framework, DDPM chooses a sequence of noise coefficients $\beta_1, \beta_2, \dots, \beta_T$ for Markov transition kernels following specific patterns. The common choices are constant schedule, linear schedule, and cosine schedule. According to [67], different

TABLE 1
Notions in Diffusion Systems

Notations	Descriptions
T	Discrete total time steps
t	Random time t
z_t	Random noise with normal distribution
ϵ	Random noise with normal distribution
N	Normal distribution
β	Generalized process noise scale
β_t	Variance scale coefficients
$\beta(t)$	Continuous-time β_t
σ	Generalized process noise scale
σ_t	Noise scale of perturbation
$\sigma(t)$	Continuous-time σ_t
α_t	Mean coefficient defined as $1 - \beta_t$
$\alpha(t)$	Continuous-time α_t
$\tilde{\alpha}_t$	Cumulative product of α_t
$\gamma(t)$	Signal-to-Noise ratio
η_t	Step size of annealed Langevin dynamics
x	Unperturbed data distribution
\tilde{x}	Perturbed data distribution
x_0	Starting distribution of data
x_t	Diffused data at time t
\tilde{x}_t	Partly diffused data at time t
x_T	Random noise after diffusion
$F(x, \sigma)$	Forward/Diffusion process
$R(x, \sigma)$	Reverse/Denoised process
$F_t(x_t, \sigma_t)$	Forward/Diffusion step at time t
$R_t(x_t, \sigma_t)$	Reverse/Denoised step at time t
$F_{ts}(x_t, \sigma_{ts})$	Forward/Diffusion step at time t
$R_{st}(x_s, \sigma_{st})$	Reverse/Denoised step at time t
$q(x_t x_{t-1})$	DDPM forward step at time t
$p(x_{t-1} x_t)$	DDPM reverse step at time t
$f(x, t)$	Drift coefficient of SDE
$g(t)$	Simplified diffusion coefficient of SDE
$\mathcal{D}(x, t)$	Degrader at time t in Cold Diffusion
$\mathcal{R}(x, t)$	Reconstructor at time t in Cold Diffusion
w, \tilde{w}	Standard Wiener process
$\nabla_x \log p_t(x)$	Score function w.r.t x
$\mu_\theta(x_t, t)$	Mean coefficient of reversed step
$\Sigma_\theta(x_t, t)$	Variance coefficient of reversed step
$\epsilon_\theta(x_t, t)$	Noise prediction model
$s_\theta(x)$	Score network model
L_0, L_{t-1}, L_T	Forward loss, reversed loss, decoder loss
L_{vlb}	Evidence Lower Bound
L_{vlb}^{CT}	Continuous evidence lower bound
L_{simple}	Simplified denoised diffusion loss
L_{simple}^{CT}	Continuous L_{simple}
L_{Gap}	Variational gap
L_{KID}	Kernel inception distance
$L_{Recovery}$	Recovery likelihood loss
L_{hybrid}	Hybrid diffusion loss
$L_{DDPM\&GAN}$	DPM ELBO and GAN hybrid loss
$L_{DDPM\&VAE}$	DPM ELBO and VAE hybrid loss
$L_{DDPM\&Flow}$	DPM ELBO and normalizing flow hybrid loss
L_{DSM}	Loss of denoised score matching
L_{ISM}	Loss of implicit score matching
L_{SSM}	Loss of sliced score matching
$L_{Distill}$	Diffusion distillation loss
$L_{DDPM\&Noise}$	DPM ELBO and reverse noise hybrid loss
L_{Square}	Noise square loss
$L_{Trajectory}$	Process optimization loss
$L_{DDPM\&Class}$	DPM ELBO and classification hybrid loss
θ	learnable parameters
ϕ	learnable parameters

noise schedules have no clear effects in experiments. The DDPM forward step & process are defined as:

$$F_t(x_{t-1}, \beta_t) := q(x_t | x_{t-1}) := \mathcal{N}(x_t, \sqrt{1 - \beta_t}x_{t-1}, \sqrt{\beta_t}\mathbf{I}) \quad (12)$$

By a sequence of diffusion steps from x_0 to x_T , We have the Forward/Diffusion Process:

$$F(x_0, \beta) := q(x_{1:T} | x_0) := \prod_{t=1}^T q(x_t | x_{t-1}) \quad (13)$$

DDPM Reverse Process: Given the forward process above, we define the Reverse step as the inverse step with respect to learned Gaussian transitions parameterized by θ [67]:

$$R_t(x_t, \Sigma_\theta) := p_\theta(x_{t-1} | x_t) := \mathcal{N}(x_{t-1}; \mu_\theta(x_t, t), \Sigma_\theta(x_t, t)) \quad (14)$$

By a sequence of reverse step from x_T to x_0 , we have the Reverse Process starting at $p(x_T) = \mathcal{N}(x_T; \mathbf{0}, \mathbf{I})$:

$$R(x_T, \Sigma_\theta) := p_\theta(x_{0:T}) := p(x_T) \prod_{t=1}^T p_\theta(x_{t-1} | x_t) \quad (15)$$

Consequently, the distribution $p_\theta(x_0) = \int p_\theta(x_{0:T}) dx_{1:T}$ should be the distribution of \tilde{x}_0 .

Diffusion Training Objective: By minimizing the negative log-likelihood (NLL), the minimization problem can be formulated as:

$$\begin{aligned} \mathbb{E}[-\log p_\theta(x_0)] &\leq \mathbb{E}_q \left[-\log \frac{p_\theta(x_{0:T})}{q(x_{1:T} | x_0)} \right] \\ &= \mathbb{E}_q \left[-\log p(x_T) - \sum_{t \geq 1} \log \frac{p_\theta(x_{t-1} | x_t)}{q(x_t | x_{t-1})} \right] \\ &= \mathbb{E}_q \underbrace{[D_{\text{KL}}(q(x_T | x_0) \| p(x_T))]}_{L_T} \\ &\quad + \sum_{t > 1} \underbrace{D_{\text{KL}}(q(x_{t-1} | x_t, x_0) \| p_\theta(x_{t-1} | x_t))}_{L_{t-1}} \\ &\quad \underbrace{-\log p_\theta(x_0 | x_1)}_{L_0} \\ &=: L \end{aligned} \quad (16)$$

Here we use the symbol of Ho *et al.* [67]. Denote L_T as the forward loss, which represents the divergence between the forwarding process and the distribution of random noise, which is a constant depending on variance schedule β_1, \dots, β_T ; Denote L_0 as the decode loss; Besides, denote $L_{1:T-1}$ as the reverse loss, which is the sum of divergence between posterior of forwarding step and reverses step at each step.

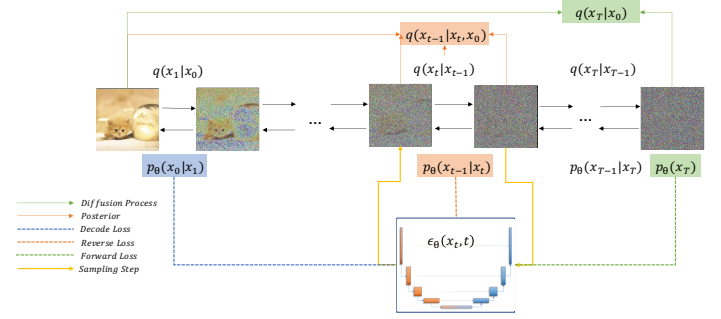


Fig. 2. Pipeline of Denoised Diffusion Probabilistic Model. The arrows pointing from left to right indicate the diffusion process and the arrows pointing in the reverse direction indicate the reverse process. The colored background transition terms are components of ELBO: the blue part stands for decode loss L_0 , the green part represents forward loss L_T , and the orange part constitutes the reverse loss L_t . Dashed lines with different colors show the training pattern of the noise prediction model ϵ_θ . Besides, in any step $1 \leq t \leq T$, the yellow lines denote the ancestral sampling process.

2.2.2 Score Matching Formulation

The score matching model aims at solving the original data distribution estimation problem by approximating the gradient of data $\nabla_x \log p(x)$, which is called score. The main approach of score matching is to train a score network x_θ to predict the score [69], [70], which is obtained by means of perturbing data with different noise schedules. The score matching process is defined as:

Score Perturbation Process & Kernel: The perturbation process consists of a sequence of perturbation steps with increasing noise scales $\sigma_1, \dots, \sigma_N$. The Gaussian perturbation kernel is defined as $q_\sigma(\tilde{x}|x) := \mathcal{N}(\tilde{x} | x, \sigma^2 \mathbf{I})$. For each noise scale σ_i , the score is equivalent to the gradient of the perturbation kernel. If we treat this increasing noise perturbation as a discrete process, the transition kernel between two neighbor states is

$$x_i = x_{i-1} + \sqrt{\sigma_i^2 - \sigma_{i-1}^2} \epsilon, \quad i = 1, \dots, N \quad (17)$$

where N is the length of the noise scale sequence, and ϵ is random noise.

Score Matching Process: As noticed above, the goal of the score matching process is to obtain a score estimation network $s_\theta(x, \sigma)$ to be as close as possible to the gradient of perturbation kernel, which is

$$L := \frac{1}{2} \mathbb{E} \left[\|s_\theta(x, \sigma) - \nabla \log q(x)\|^2 \right] \quad (18)$$

where θ is the learnable parameters in the score network.

DDPM & DSM Connection: To some extent, score matching and denoising diffusion are the same kinds of processes. (1) Denoising mechanism: both DSM and DDPM follow the pattern of fetching information during the noising process and reusing gradient during the denoising process. Both processes transform prior distribution to known noise and finally reverse back to the original distribution. Moreover, noising schedule of DSM can be seen as an accumulation of

constant-variance diffusion steps. (2) Training object: Both DSM and DDPM aim at maximizing the prior likelihood and they train the network for gradient prediction. (3) Sampling method: both DSM and DDPM apply the idea of ancestral sampling, reconstructing the samples by collecting related gradients step by step.

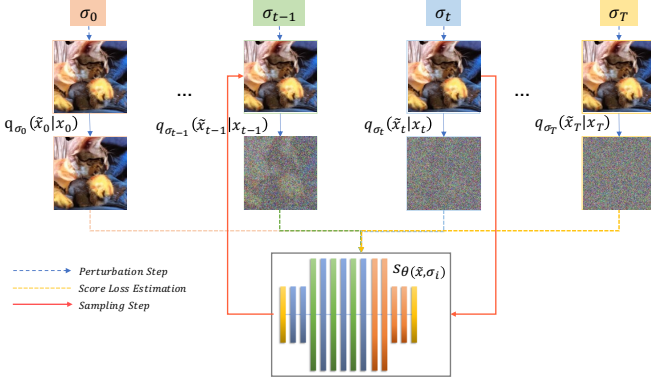


Fig. 3. Pipeline of Denoised Score Matching (DSM). The σ 's in different time states on the top represent alternative scales of noise. The transition states $p_{\sigma_t}(\tilde{x}_t | x_t)$ are the output gradients of the perturbation. Dashed lines with different colors reveal that the scoring network s_θ is trained by minimizing the sum of L2-loss between the output gradient and the score in each noise scale. Besides, in any noise state $1 \leq t \leq T$, the red lines denote the Langevin Dynamics sampling process.

2.2.3 Score SDE Formulation

Score SDE [65] proposed a unified continuous framework based on the stochastic differential equation to describe diffusion models and denoised score matching models. It not only presents the corresponding continuous set-up of DDPM of DSM based on score SDE but also proposes a density estimation ODE framework named probability flow ODE.

Forward Score SDE Process: In Song *et al.* [65], Diffusion process can be viewed as a continuous case described by Stochastic Differential Equation. And it is equal to the solution to Itô SDE [71], which is composed of a drift part for mean transformation and a diffusion coefficient for noise description. :

$$dx = f(x, t)dt + g(t)dw, t \in [0, T] \quad (19)$$

where w is the standard Wiener process/Brownian Motion, $f(\cdot, t)$ is the drift coefficient of $x(t)$, and $g(\cdot)$ is the simplified version of diffusion coefficient of $x(t)$, which is assumed not dependent on x . Besides, $p_0, p_t(x)$ denote the data distribution and probability density of $x(t)$. p_T denotes the original prior distribution which gains no information from p_0 . When the coefficients are piece-wise continuous, the forward SDE equation admits a unique solution [72].

Similar to the discrete case, the forward transition in the SDE framework is derived as:

$$\begin{aligned} F_{st}(x(s), g_{st}) &:= q(x_t | x_s) := \mathcal{N}\left(x_t | f_{ts}x_s, g_{ts}^2 I\right) \\ R_{ts}(x(t), g_{ts}) &:= q(x_s | x_t, x_0) \\ &= \mathcal{N}\left(x_s | \frac{1}{g_{t0}^2} \left(f_{s0}g_{ts}^2 x_0 + f_{ts}g_{s0}^2 x_t \right), \frac{g_{s0}^2 g_{ts}^2}{g_{t0}^2} I\right) \end{aligned} \quad (20)$$

$$\text{where } f_{ts} = \frac{f(x, t)}{f(x, s)} \text{ and } g_{ts} = \sqrt{g(t)^2 - f_{ts}^2 g(s)^2}.$$

Reversed Score SDE Process: In contrast to the Forward SDE Process, the Reversed SDE Process is defined with respect to the reverse-time Stochastic Differential Equation by running backward in time [65]:

$$dx = [f(x, t) - g(t)^2 \nabla_x \log p_t(x)] dt + g(t)d\bar{w}, t \in [0, T] \quad (21)$$

Furthermore, $\nabla_x \log p_t(x)$ is the score to be matched [73].

Score SDE Training Objective: The training objective of score SDE employs weighting scheme in the score loss compared to denoised score matching, which is

$$L := \mathbb{E}_t \{ \lambda(t) \mathbb{E}_{x(0)} \mathbb{E}_{x(t)x(0)} [\|s_\theta(x(t), t) - \nabla_{x(t)} \log p(x(t)x(0))\|_2^2] \} \quad (22)$$

where $x(t), x(0)$ are corresponding continuous time variables of x_t, x_0 .

SDE-based DDPM & DSM: Based on the SDE frameworks, the transition kernel of DDPM and DSM can be expressed as :

$$dx = -\frac{1}{2} \beta(t) x dt + \sqrt{\beta(t)} dw \quad (23)$$

$$dx = \sqrt{\frac{d[\sigma^2(t)]}{dt}} dw \quad (24)$$

where $\beta(t)$ and $\sigma(t)$ are the continuous-time variable of discrete noise scales β_t and σ_t . Moreover, the two kinds of SDE are called Variation Preserving (VP) and Variation Explosion (VE) SDE respectively.

Probability Flow ODE: Probability Flow ODE (Diffusion ODE) [65] is the continuous-time ODE that supports the deterministic process which shares the same marginal probability density with SDE. Inspired by Maoutsa *et al.* [74] and Chen *et al.* [75], any type of diffusion process can be derived into a special form of ODE. In the case that functions G is independent of x , the probability flow ODE is

$$dx = \{f(x, t) - \frac{1}{2} G(t) G(t)^T \nabla_x \log p_t(x)\} dt \quad (25)$$

In contrast to SDE, probability flow ODE can be solved with larger step sizes as they have no randomness. Due to the advantages of ODE, several works such as PNDMs [76] and DPM-Solver [63] obtain amazing results by modeling the diffusion problem as an ODE.

2.3 Training Strategy

2.3.1 Denoising Diffusion Training Strategy

In order to minimize the negative log-likelihood, the only item we can be used to train is $L_{1:T-1}$. By parameterizing the posterior $q(x_{t-1}|x_t, x_0)$ using Baye's rule, we have:

$$q(x_{t-1} | x_t, x_0) = \mathcal{N}(x_{t-1}; \tilde{\mu}_t(x_t, x_0), \tilde{\beta}_t I) \quad (26)$$

where α_t is defined as $1 - \beta_t$, $\bar{\alpha}_t$ is defined as $\prod_{k=1}^t \alpha_k$. Mean and variance schedules can be expressed as:

$$\begin{aligned} \tilde{\mu}_t(x_t, x_0) &:= \frac{\sqrt{\alpha_{t-1}} \beta_t}{1 - \bar{\alpha}_t} x_0 + \frac{\sqrt{\alpha_t} (1 - \bar{\alpha}_{t-1})}{1 - \bar{\alpha}_t} x_t \\ \tilde{\beta}_t &:= \frac{1 - \bar{\alpha}_{t-1}}{1 - \bar{\alpha}_t} \beta_t \end{aligned} \quad (27)$$

Keeping above parameterization as well as reparameterizing x_t as $x_t(x_0, \sigma)$, L_{t-1} can be regarded as an expectation of L2-loss between two mean coefficients:

$$L_{t-1} = \mathbb{E}_q \left[\frac{1}{2\sigma_t^2} \|\tilde{\mu}_t(x_t, x_0) - \mu_\theta(x_t, t)\|^2 \right] + C \quad (28)$$

Simplifying L_{t-1} by reparameterizing μ_θ w.r.t ϵ_θ , we obtain the simplified training objective named L_{simple} :

$$L_{simple} := \mathbb{E}_{x_0, \epsilon} \left[\frac{\beta_t^2}{2\sigma_t^2 \alpha_t (1 - \bar{\alpha}_t)} \right] \|\epsilon - \epsilon_\theta(\sqrt{\bar{\alpha}_t} x_0 + \sqrt{1 - \bar{\alpha}_t} \epsilon)\|^2 \quad (29)$$

Most diffusion models until now use the training strategy of DDPMs. But there exist some exceptions. DDIM's training objective can be transformed by adding a constant from DDPM's although it is independent of Markovian step assumption; Training pattern of Improved DDPM named as L_{hybrid} is to combine training object of DDPM L_{simple} and a term with variational lower bound L_{vlb} . However, L_{simple} still takes the main effect of these training methods.

2.3.2 Score Matching Training Strategy

Traditional score matching techniques requires massive computation cost for Hessian of log density function. To fix this problem, advanced methods find approaches to avoid Hessian computing. Implicit score matching (ISM) [73] treat the real score density as a non-normalized density function that can be optimized by neural network. Sliced score matching (SSM) [77] provide a unperturbed score estimation method through reverse-mode auto-differentiation by projecting score onto random vectors.

$$L_{ISM} := \mathbb{E} \left[\frac{1}{2} \|s_\theta(x)\|_\Lambda^2 + \nabla(s_\theta) \right] \quad (30)$$

$$L_{SSM} := \mathbb{E}_p \mathbb{E}_{P_{data}} \left[v^\top \nabla_x s_\theta(x) v + \frac{1}{2} \|s_\theta(x)\|_2^2 \right] \quad (31)$$

However, because of the low-manifold problem in real data as well as the sampling problem in the low-density region, denoised score matching could be the better solution for improving score matching. Denoised score matching (DSM) [69] transforms the original score matching into a perturbation kernel learning by perturbing a sequence of increasing noise.

$$L_{DSM} := \frac{1}{2} \mathbb{E}_{q_\sigma((\tilde{x}|x)p_{data}(x))} \left[\|s_\theta(\tilde{x}) - \nabla_{\tilde{x}} \log q_\sigma(\tilde{x}|x)\|_2^2 \right] \quad (32)$$

According to Song *et al.*, the noise distribution is defined to be $q_\sigma(\tilde{x}|x) = \mathcal{N}(\tilde{x}|x, \sigma^2 I)$. Thus, for each given σ , the specific expression denoising score matching objective is

$$L(\theta; \sigma) := \frac{1}{2} \mathbb{E}_{p_{data}(x)} \mathbb{E}_{\tilde{x} \sim \mathcal{N}(x, \sigma^2 I)} \left[\left\| s_\theta(\tilde{x}, \sigma) + \frac{\tilde{x} - x}{\sigma^2} \right\|_2^2 \right] \quad (33)$$

2.4 Sampling Algorithm

Reconstructing data distribution needs sampling. In each sampling step, the sample generated from random noise will be refined again to get closer to the original distribution. In this subsection, we present basic sampling algorithms for the three landmark works.

2.4.1 Ancestral Sampling

The initial idea of ancestral sampling [78] is reconstructed with the gradient of inverse Markovian step by step.

2.4.2 Langevin Dynamics Sampling

With a fixed step size $\epsilon > 0$, Langevin dynamics can produce samples from a probability density $p(x)$ through only the score function (Song *et al.*) $\nabla_x \log p(x)$.

2.4.3 Predictor-corrector (PC) Sampling

PC sampling [79] is inspired by a type of ODE black-box ODE solver [80], [81], [82] in order to produce high-quality samples and trade-off accuracy for efficiency for all reversed SDE. The sampling procedure comprises a predictor sampler and a corrector sampler.

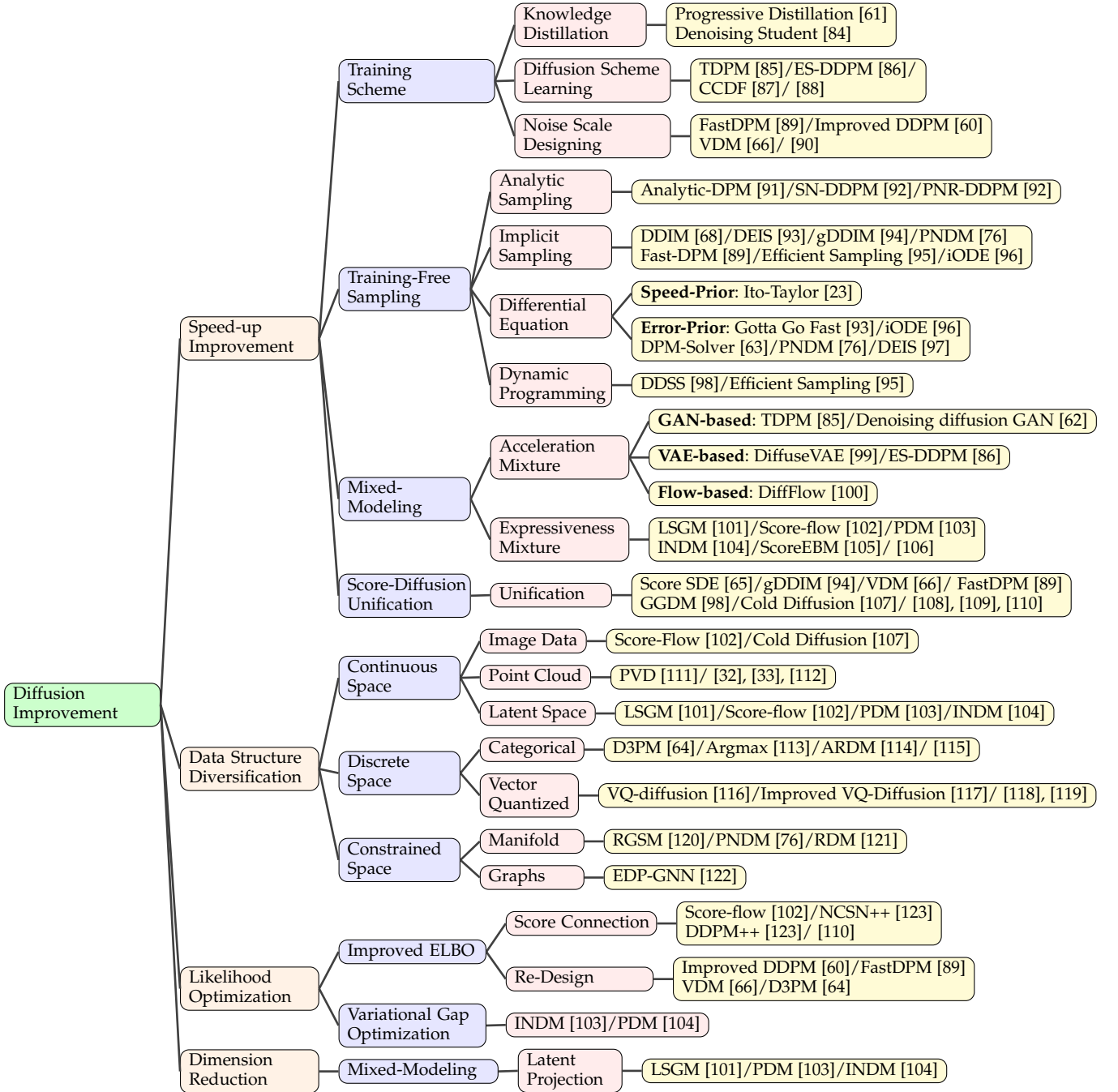
3 ALGORITHM IMPROVEMENT

Nowadays, the main concern of the diffusion model is to speed up its speed and reduce the cost of computing. With the aid of strongly conditioned settings, diffusion sampling can be achieved in just a few steps [42], [61], [83]. In general cases, it takes thousands of steps for diffusion models to generate a high-quality sample. Mainly focusing on improving sampling speed, many works from different aspects come into reality. Besides, handling a diverse range of data for wider applications, optimizing log-likelihood by ELBO-based expressiveness models, and reducing computation cost and time with dimension reduction techniques still count. In this section, we divide the improved algorithm w.r.t. problems to be solved. For each problem, we present the significance and related detailed classification of improved techniques.

3.1 Speed-up Improvement

Although diffusion models enjoy a strong generative ability with high tractability, long sampling steps and slow sampling speed limit models' practicality. To improve this situation, advanced techniques can be divided into four categories including training scheme enhancement, training-free accelerated sampling, mix-modeling design, and score-diffusion unification design.

TABLE 2
Classification of Improved Diffusion Techniques



3.1.1 Training Schedule

The improvement in the training schedule means changing traditional ways of training such as diffusion schemes, and noise schemes, which are independent of sampling. Recent studies have shown the key factors in training schemes influencing learning patterns and models' performance. Thus, in this sub-section, we divide the training enhancement into three categories: knowledge distillation, diffusion scheme learning, and noise scale designing.

Knowledge Distillation Knowledge distillation is an emerging method for obtaining efficient small-scale net-

works by transferring "knowledge" from complex teacher models with high learning capacity to simple student models [124], [125]. Thus, student models equip the advantages in model compression and model acceleration [126], [127], [128], [129].

Salimans *et al.* [61] firstly utilize the core idea into diffusion model improvement by progressively distilling knowledge from one sampling model to another. In each distillation step, student models re-weight from teacher models before being trained to generate one-step samples as close as teacher models do. Consequently, student models halve their sampling steps during each distillation process.

Following the same training objective as DDPMs with alternative parameterization methods, the Progressive Distillation model achieved an FID of 2.57 in only four steps. This core idea was used for text-to-speech generation in ProDiff [130]. Unlike progressive distillation, denoising students directly distill knowledge from scratch by minimizing KL Divergence between two categorical distributions.

Diffusion Scheme Learning Diffusion sampling is partly determined by the forward process. Thus, learning an efficient diffusion process to optimize the reverse process indirectly is a valid approach to achieve speed-up improvement.

Recent studies focus on analyzing diffusion steps. From a theoretical perspective of ELBO minimization, CCDF [87] and Franzese *et al.*, [88] establish an optimization problem where number diffusion step is treated as a variable for minimizing ELBO. Special techniques such as contraction theory [131] and gap function [132] are employed in the analysis. Another perspective is based on truncation. The key idea of truncating patterns is generating less diffused data with the help of other generative models like GAN and VAE. TDPM [85] truncates both diffusion and sampling processes by sampling from implicit generative distribution learned by GAN and conditional transport (CT) [133]. Similarly, Early Stop (ES) DDPM [86] learns from latent space to generate implicit distributions. Compared to theoretical analysis, the truncation process deals with a trade-off between generating speed and sample quality. Since generated samples differ between diffusion and other generative models, probing an optimized truncated ratio practically is required.

Noise Scale Designing In both diffusion and reverse processes, each noise injection step can be regarded as a random walk on the trajectory, indicating that noise scale learning may guide a reasonable noising and regular sampling. Thus, regularizing diffusion and sampling steps by designing variance and noise scales guides fast convergence. Existing methods treating noise scale as a learnable parameter contain forward noise design and reverse noise design.

Among the forward noise design method, VDM [66] reparameterized the noise scalar as signal-to-noise ratio to directly connect noise scale, pointing out that noise scale design determines model type and model performance. FastDPM [89] obtains forward noise from time step or variance scalar, connecting noise design to ELBO optimization. In the reverse noise design methods, improved DDPM [60] learns the reverse noise scale implicit by training a hybrid loss containing L_{simple} and L_{vlb} . Besides, San Roman *et al.* employs a noise prediction network to update the reverse noise scale directly before conducting ancestral sampling in each step.

3.1.2 Training-Free Sampling

Many methods are focusing on changing the pattern of training and noise schemes to improve sampling speed, but re-training models cost additional computing and lead to the risk of unstable training. Thankfully, there exists a class of methods that directly enhance the sampling algorithm with pre-trained models called training-free sampling. Advanced training-free sampling aims to propose an efficient sampling algorithm for acquiring knowledge

from the pre-trained models with fewer steps and higher accuracy. It contains four categories: analytical methods, implicit sampler, differential equation solver sampler, and dynamic programming adjustment.

Analytical Method Existing training-free sampling methods take reverse covariance scales as a hand-crafted sequence of noises without considering the states. Analytical methods are proposed by Bao *et al.* [91] for solving covariance optimization problems to dynamically conducting sampling steps. Analytic-DPM [91] accomplishes reverse noise selection based on assuming the reverse means in each step. For the situations where the optimized reverse means are not given, there requires a correction of mean and covariance. Extend analytic-DPM [92] makes further noise correction by another noise prediction network on pre-trained DDPM models.

Implicit Sampler The implicit sampler is a class of jump-step samplers that do not require diffusion model re-training. Usually, it takes the same number of steps for the generative process as the diffusion process to rebuild the original data distribution in DDPM. However, the diffusion model has the so-called decoupling property that does not require the equivalent number of steps for diffusing and sampling. Inspired by generative implicit model [134], Song *et al.*, [68] has proposed implicit sampling method equipped with deterministic diffusion and jump-step sampling. DDIM first solves the jump-step acceleration using continuous process formulation [75], [135] with the aid of neural ODE as:

$$d\bar{x}(t) = \epsilon_{\theta}^{(t)} \left(\frac{\bar{x}(t)}{\sqrt{\sigma^2 + 1}} \right) d\sigma(t) \quad (34)$$

where σ_t is parameterized by $\sqrt{1 - \alpha}/\sqrt{\alpha}$, and \bar{x} is parameterized as $x/\sqrt{\alpha}$. Besides, the probability can be treated as one kind of Score SDE, which is derived from the discrete formulation:

$$\frac{x_{t-\Delta t}}{\sqrt{\alpha_{t-\Delta t}}} = \frac{x_t}{\sqrt{\alpha_t}} + \left(\sqrt{\frac{1 - \alpha_{t-\Delta t}}{\alpha_{t-\Delta t}}} - \sqrt{\frac{1 - \alpha_t}{\alpha_t}} \right) \epsilon_{\theta}^{(t)} (x_t) \quad (35)$$

Following the discrete formulation of DDIM, FastDPM [89] improves the sampling algorithm by re-designing the reverse noise schedule. Furthermore, since DDIM is regarded as one type of probability flow ODE [75], many ODE-solver enhancement works are applicable to implicit solver acceleration. Not limited to employing high-order ODE-solver as PNDM [76] and iODE [96], DEIS [136] and DPM-solver [63] reformulate probability flow ODE as semi-linear ODE to improve sampling speed. Apart from the above two improved routes, the dynamic programming sampling algorithm with jump-step property proposed by Watson *et al.* can be viewed as one type of implicit sampler.

Based on the above improved implicit sampler, gDDIM [94] generalized them with diverse types of kernels in the SDE framework including DDPM, DDIM, and critically-damped Langevin diffusion (CLD) [137] into a family of DDIM, achieving implicit diffusion model acceleration by a multi-step exponential sampler. Implicit diffusion holds a wider

enhancement space due to its differential equation formulation and jump-step mechanism. Further methods with fewer sampling steps and plausible theoretical constraints such as the manifold hypothesis and the sparsity property are to be explored.

Differential Equation Solver Sampler Differential Equation (DE) Solver Sampler is a class of solvers for ODE-based and SDE-based formulations to minimize approximation error during diffusion sampling. Inspired by Score SDE [65], obtaining high-quality samples is a differential equation-solving process with numerical solvers. Thus, with the aid of existing fast and stable ODE/SDE solvers, differential-based methods draw increasing attention nowadays due to their concise formulation and the vast range of solvers. [138], [139] Generally, there are two basic DE formulations: SDE formulation enjoys randomness when walking in the direction field; ODE formulation with deterministic property enjoys faster speed. [23] As for the DE solvers [140], [141], [142], [143], higher-order DE solvers have smaller approximation errors and higher order of convergence, it requires more evaluations [144] and suffers from instability issues. In this subsection, we introduce the current algorithms based on the trade-off of different frameworks and DE solvers. We divide them into speed-prior and accuracy-prior.

For the methods preferred accuracy leveraging higher order solver, Itô-Taylor Sampling Scheme [97] has been proposed using a high-order SDE solver. Besides, ideal derivative substitution is applied to parameterize the score function in a tricky way that avoids higher-order derivative computing. The speed-prior methods to improve the whole process by applying both linear solvers and higher-order solvers include Gotta Go Fast [93], iODE [96], and PNDM [76]. Gotta Go Fast achieves an algorithm based on directional guidance on step size adjustment. The sampling process combines a linear solver (Euler-Maruyama Method) with a higher-order one (Improved Euler Method) with an extrapolation technique to accelerate with less extra computing. iODE employs second-order Heun's solver along with adjusted time steps on deterministic diffusion ODE. PNDM has explored that different numerical solvers can share the same gradient, leading to exploring the linear multi-step method after using three steps of a higher-order solver (Runge-Kutta method) in Diffusion ODE. Besides, DPM-solver [63] also leveraged solvers of different orders. Empirically, DPM Solver-Fast (progress with a mixture of different order solvers) performed the best among all the choices. Therefore, a united solver cross alternative orders may perform better after well-design.

Furthermore, from the perspective of differential equation formulation, DPM-solver and DEIS [93] created a new viewpoint except for SDE and Diffusion ODE. The trade-off extrusion ODE can be seen as a semi-linear form by which the discretization errors are reduced. On the other hand, DEIS improved numerical DDIM with a multi-step PC-sampling method [136] with exponential integrator [145]. Currently, semi-linear-based ODE performs the best but still requires other techniques, such as threshold limit [93], and analytical form [63].

Dynamic Programming Adjustment Dynamic programming (DP) achieves the traversal of all choices to find the optimized solution in a reduced time by memorization trick [146], [147], [148], [149]. Compared to other efficient sampling, methods with dynamic programming locate the optimized sampling route instead of designing powerful steps that minimize the error within less time. Assume that each path from one state to another shares the same KL-Divergence with others, Watson *et al.*, [95] proposed an efficient sampling method to directly search the optimized route of sampling with the minimum ELBO. This method only requires $\mathcal{O}(T^2)$ for computing and restoration, and it explores a new approach for optimizing the trajectory. However, the minimization on ELBO sometimes has a mismatch with FID scores [150]. Inspired by Kumar *et al.*, [151] differentiable Diffusion Sampler Search (DDSS) [98] utilizes rematerialization trick to trade memory cost for computation time. Current DP methods concerning ELBO and noise as optimizing objectives, time step oriented and sample quality (distance) oriented methods may have promising achievements.

3.1.3 Mixed-Modeling

Mixed-modeling stands for extending different types of generative models to combine their strengths [152], [153], [154], [155], [156], [157], [158]. For diffusion mixed-modeling, diffusion models take virtue of high-speed sampling of others (such as adversarial training network and auto-regressive encoder) and high expressiveness (such as normalizing flow). Thus, extracting all the strengths by jointly combining two or more models with a specific pattern not only performs a promising enhancement but also helps perceive connections between diffusion models and others. Mixed modeling can be classified into two classes from the perspective of mixing purpose: acceleration mixture and expressiveness mixture.

Acceleration Mixture Acceleration mixture aims at applying high-speed generation of VAEs and GANs to save plenty of steps on the reconstruction of less perturbed data distribution. Existing GAN-based methods consist of two parts as previous GAN related works: the generator generates samples x'_0 to be diffused into x'_{t-1} which is as close as x_{t-1} , while the discriminator distinguishes x'_{t-1} and x_{t-1} under the condition of x_t along with $q(x_t|x_{t-1})$. Denoised diffusion GAN [62] became the first DDPM-related model that generated samples with 4 steps. Following a similar pattern, VAE-based models like DiffuseVAE [99] and ESDDPM [86] apply. Since it takes much time to predict x_0 in each sampling step when we use $q(x_{t-1}|x_t, x_0)$, VAEs are used in x_0 generation to accelerate the whole process, which is what DiffuseVAE has done. Based on DiffuseVAE, ESDDPM combined the early stop idea in sample trajectory learning and DiffuseVAE to accomplish early stop sampling with the condition generated from diffused VAE samples.

Expressiveness Mixture Another category of mixed-modeling called expressiveness mixture support diffusion models on expressing data or noise in a different pattern. High-expressiveness data combined with speed-up techniques achieve speed-up by saving computation costs. The

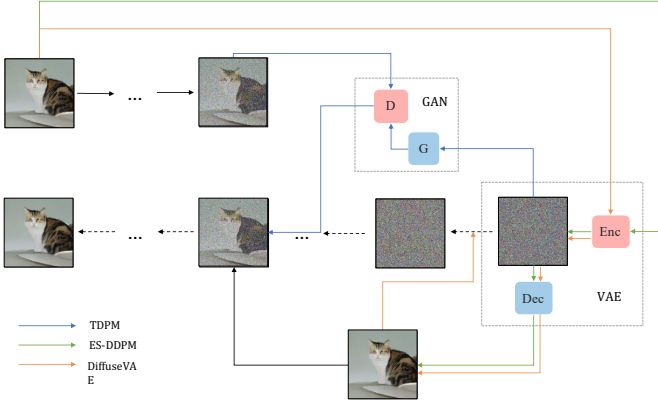


Fig. 4. Acceleration mixed-modeling pipeline. The blue line represents the pipeline of TDPM. The partly perturbed data x_t is applied as the ground-truth condition for GAN's generator, and the conditional samples x'_t with the same perturbation level are generated from the latent before being compared with x_t . The successful samples are applied as the beginning of the reverse process. Instead of using GAN as the high-speed generator, ES-DDPM follows the pattern of TDPM's with VAE, shown with green lines. Besides, DiffuseVAE employs VAE to generate condition \hat{x}_0 in each sampling step.

high expressiveness methods can be divided into noise modulation, space projection, and kernel expressiveness. As for noise modulation, DiffFlow [100] employs a flow function in each SDE-based diffusion step forward and backward to add noise adaptively and efficiently by minimizing the KL-Divergence between the forward process and backward process. DiffFlow leads to a 20* speedup compared to DDPM, although there is a longer time required per step since the flow functions' back-propagation. Space projection methods leverage NFs into data transformation. Space projection methods benefit from specific spaces' properties implemented by projecting models. Both LSGM [101] and PDM [103] obtained latent variables using VAE and flow function respectively to take advantages of fast computing. Besides, Score-Flow [102] employs normalizing flow to transform data distribution into a dequantization field and conduct a diffusion process to generate dequantized samples. Projecting data onto the dequantization field with variational dequantization solves the mismatching between continuous density and discrete data [159], [160], eliminating the gap between dequantization space and discrete space. Another type of expressiveness mix-modeling based on an energy-based model [161], [162], [163], [164] takes the virtue of expressive flexibility of energy function [105] on reverse transition kernel.

3.1.4 Score & Diffusion Unification

Based on diffusion models and denoised score matching methods, Score SDE [65] builds a unified continuous framework linking diffusion and perturbation processes to provide a universal tool for related tasks. Score-diffusion unification models work since the insight from landmark unification helps in exploring efficient sampling mechanisms. Furthermore, generalized works provide multi-view for benefiting diffusion models. There are two categories of works: generalized works that reformulate diffusion-based models, and unified works that connect score and diffusion networks.

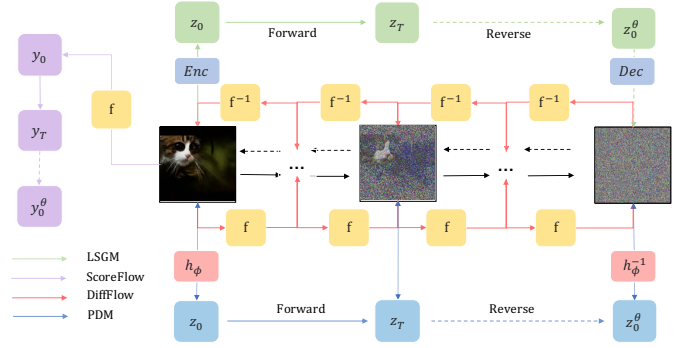


Fig. 5. Expressiveness mixed-modeling pipeline. The models for expressiveness enhancement keep the same procedure as DDPM in the training, diffusion, and sampling process, denoted by black lines. Furthermore, additional improvements are highlighted by other colors. The red lines show the pipeline of DiffFlow, which adds a flow function and related inverse function at each step. The works in blue and green lines represent the idea of latent space diffusion by jointly training mixture models. Different supporting generative models are used in LSGM and PDM. Besides, Score-Flow uses the flow function as a projector from discrete to dequantization space. Then generating dequantized samples using the traditional diffusion method.

For generalized perspective, FastDPM [89] and VDM [66] finished the unification w.r.t. noise schedules by noise-time bijective map and signal-to-noise ratio respectively. Both methods analyze training and sampling schemes with re-defined variables. Generalized DDIM (gDDIM) [94] unifies the DDIM family according to the transition kernel during each step, benefiting implicit acceleration from the bottom.

From the unification perspective Gong *et al.*, [109] reveals the hidden connection between score matching with the normalizing flow, and it provides a new approach to expressing score matching by flow ODEs [75], [135]. Bortoli *et al.*, [108] provided a variational score matching approach for simulating diffusion bridges using Doob-h transformation [165]. GGDM [95] generalizes diffusion models with non-Markovian samplers and a vast range of marginal variance to explore formulations of a wider diffusion family. Cold diffusion [107] view diverse forward and reversed kernels as unified ones, extending prior distribution to any time. Huang *et al.* [110] presents a variational form for likelihood estimation, enhancing theoretical support for variational gap minimization.

3.2 Data Structure Diversification

Currently, most improvement methods for acceleration and computation cost reduction concentrate on the performance of RGB-image data in order to evaluate the power of generation. Indeed, most kinds of existing data can be the input of diffusion models, leading to various applications in the other fields, such as amino acid residue [55], audio sequence [47], and torsion angle [54]. More importantly, the traditional patterns of diffusion which utilize Gaussian distribution as prior and transition kernel are to be extended to explore the influences of patterns with distinct distributions. To improve diffusion model's generalization ability, we divided the distribution diversification into three aspects: discrete space, continuous space, and Constrained space with structural constraints.

3.2.1 Continuous Space

As mentioned above, dequantization space projection solves the mismatching between continuous density and discrete data [159], [160] as well as eliminates the gap between dequantization space and discrete space [27], [166]. Point cloud data used for 3d shape generation, 3d shape completion, and multi-modal completion attract more attention [167], [168] but meet the barrier using the autoregressive encoder and normalizing flows due to the irregular sampling procedure. For continuous space methods, two main classes - image space and point cloud space are introduced. Space generalization is accomplished by projection networks such as VAE and normalizing flow for data transformation.

Image & Point Cloud Score-flow [102] employs a flow function to project RGB-image into dequantization space, achieving diffusion techniques for generating accurate samples. Cold diffusion [107] projects image into any type of distribution, eliminating the prediction error by the wrong design of Reconstructor \mathcal{R} (Generalized term of all types of the samplers).

Point cloud generation is firstly proposed by Luo *et al.* [32], which generates latent samples for point cloud data, and conducts transformation to obtain high-quality 3d shapes. Other techniques such as [33], [111], [112] accomplish the shape generation and completion tasks in similar ways. Some slight improvements used in latent space transformation such as canonical map [112], condition feature extraction sub-nets [33], and point-voxel representation [111].

Latent Space Similar to Expressiveness mixture modeling, latent space data distributions are often processed for diffusion application since different types of complex data structures require a unified approach to generalize and analyze. Most current methods project data into continuous space, and they obtain promising performance with the aid of high-quality generation power of diffusion models such as EDM [21] and antigen-diffusion [22]. Thus, latent space processing should be a beneficial pattern utilized in new application fields.

3.2.2 Discrete Space

Deep generative models have many significant achievements in natural language processing [169], [170], multi-modal learning [171], [172], and AI for science [173], [174] with relevant architectures and advanced techniques. Among these successes, processing discrete data such as sentences, residue, atom, and vector-quantized data is necessary for eliminating inductive bias. Thus, based on the previous fortune, conducting relevant tasks with diffusion models hold promising foreground. We divide the main problem into processing text & categorical data and vector-quantized data.

Text & Categorical To process categorical features, D3PM [64] firstly promoted diffusion algorithm onto discrete space to deal with discrete data like sentences and images by means of defining

$$q(x_t | x_{t-1}) = \text{Cat}(x_t; p = x_{t-1} \mathcal{Q}_t) \quad (36)$$

where $[\mathcal{Q}_t]_{ij} = q(x_t = j | x_{t-1} = i)$ is defined as the transition, and $\text{Cat}(\cdot)$ is defined as the categorical distribution over the one-hot row vector.

Similar to D3PM, multi-nomial diffusion [113] and ARDM [114] extended the categorical diffusion into multi-nomial data for generating language text & segmentation map and Lossless Compression.

Vector-Quantized To handle the multi-model problem, vector-quantized (VQ) data is proposed to combine data from different fields into the codebook. VQ data processing achieved great performance in autoregressive encoders [175]. Gu *et al.* [116] firstly applied diffusion techniques into VQ data, solving unidirectional bias as well as accumulation prediction error problems existing in VQ-VAE. Further works such as Xie *et al.* [119], Cohen *et al.* [118], and Improved VQ-Diffusion [117] accomplished text-to-sign pose generation, diffusion-bridge generation through VQ-VAE pipeline, and inference strategy improvement respectively by re-defining the transition process as:

$$q(x_t | x_{t-1}) = v^\top(x_t) \mathcal{Q}_t v(x_{t-1}) \quad (37)$$

where $v(t)$ is a one-hot vector of the equal length with the code-book, and $\mathcal{Q}(t)$ is called the probability transition matrix:

$$\mathcal{Q}_t = \begin{bmatrix} \alpha_t + \beta_t & \beta_t & \beta_t & \cdots & 0 \\ \beta_t & \alpha_t + \beta_t & \beta_t & \cdots & 0 \\ \beta_t & \beta_t & \alpha_t + \beta_t & \cdots & 0 \\ \vdots & \vdots & \vdots & \ddots & \vdots \\ \gamma_t & \gamma_t & \gamma_t & \cdots & 1 \end{bmatrix} \quad (38)$$

Training methods are similar to DDPM's but with a new expression scheme.

3.2.3 Constrained Space

Graph-based neural networks step over traditional data constraints and re-express latent connections among existing data such as social networks [176], [177], molecular [178], [179], and weather conditions [180], [181]. Moreover, manifold learning methods hold the advantages of non-redundant expression and comprehensive portrayals, such as protein and RNA. Thus, constrained space extension methods are based on the Riemann manifold and graph.

Manifold Space Most current data structures such as images and text are defined in Euclidean space, which is a flat-geometry manifold. However, there exists a series of data in the field of robotics [182], geoscience [?], [183], and protein modeling [184] defined in Riemannian manifold [185], where existing methods for Euclidean space cannot capture the feature of sphere well. Thus, recent methods RDM [121] and RGSM [120] applied diffusion techniques into Riemannian manifold by score SDE framework [65] with a slight change.

Unlike the above two methods, PNDM [76] draws support from Manifold space to solve the neural differential equation for sampling, which indeed is a generalized version for differential equation sampler [186].

Graph According to [187], graph is becoming an increasingly popular topic but few works are proposed in the field of diffusion. In EDP-GNN [122], graph data is processed through an adjacency matrix before being applied in the traditional discrete score matching pipeline to capture the graph's permutation invariance.

3.3 Likelihood Optimization

Most variational methods [175], [188] and diffusion methods [67] train models by the principle of variational evidence lower bound (ELBO) since the log-likelihood is not tractable. However, sometimes the log-likelihood is still not competitive because the variational gap between ELBO and log-likelihood is not minimized at the same time. Thus, several methods [60], [102] directly focus on the likelihood optimization problem to solve this problem. The solutions can be classified into two classes – improved ELBO and variational gap optimization.

3.3.1 Improved ELBO

Based on the original ELBO, many works try to tighten the lower bound to make log-likelihood more competitive. There are two types of approaches: score connection and re-design.

Score Connection: Inspired by [189], [190], score connection methods provide a new connection between ELBO optimization and score matching, solving the likelihood optimization problems via improved score training. Score-flow [102] treats the forward KL divergence in ELBO as optimizing a score matching loss with a weighted scheme. Huang *et al.* [110] treated Brownian motion as a latent variable to track the log-likelihood estimation explicitly, and it builds the bridge between the estimation and weighted score matching in the variational framework. Similarly, NCSN++ [123] bridges the theoretical gap by introducing a truncation factor to ELBO.

Re-Design: Compared to loss transformation techniques, re-Design methods directly tighten the ELBO by re-designing noise scale and training objectives. VDM [66] and DDPM++ [123] connect the advanced training objectives with respect to signal-to-noise ratio and truncate factors respectively, optimizing ELBO via finding optimal factors. Improved DDPM [60] and D3PM [64] propose hybrid loss functions based on ELBO with a weighted scheme for improving ELBO.

$$L_{\text{hybrid}} = L_{\text{simple}} + \lambda L_{\text{vlb}} \quad (39)$$

3.3.2 Variational Gap Optimization:

Apart from designing advanced ELBO, minimizing the variational gap is still one approach to maximize the log-likelihood. Based on the success of variational gap optimization [191] in the VAE field, INDM [103] applies the flow model to express the variational gap, minimizing the gap by jointly training the bidirectional flow model and linear diffusion model on latent space. Additionally, PDM accomplishes the variational gap expression by introducing encoder loss of VAE. With collective training, a unique optimal solution exists to eliminate the gap.

3.4 Dimension Reduction

Unlike the variational auto-encoder that projects data into the latent lower dimension, computing the high-dimensional dataset is extremely consuming during training and sampling. However, existing diffusion-based models are based on transition kernels on equivalent spaces, which leads to the disability of dimension reduction. Thus, with the aid of dimension-reduction models such as normalizing flows and VAEs, mix-modeling problems that improve model expressiveness show promising potential to fix this problem.

Latent Projection Several mix-modeling methods project training data onto the latent space with a lower dimension by flow function and VAE-encoder, conducting diffusion and denoising processes. LSGM [101], INDM [104] and PDM [103] follow the pattern so as to learn smoother models in a smaller space, triggering fewer network evaluations and faster sampling [101]. Furthermore, weighting training techniques that use joint training of both diffusion models and projecting models based on ELBO maximization and log-likelihood maximization are employed.

4 APPLICATION

Benefiting from the powerful ability to generate realistic samples, diffusion models have been widely used in various fields such as computer vision, natural language processing, and bioinformatics.

4.1 Computer vision

4.1.1 Low-level vision

CMDE [26] empirically compared score-based diffusion methods in modeling conditional distributions of visual image data and introduced a multi-speed diffusion framework. By leveraging the controllable diffusion speed of the condition, CMDE outperformed the vanilla conditional denoising estimator [69] in terms of FID scores in in-painting and super-resolution tasks. DDRM [192] proposed an efficient, unsupervised posterior sampling method served for image restoration. Motivated by variational inference, DDRM demonstrated successful applications in super-resolution, deblurring, inpainting, and colorization of diffusion models. Palette [83] further developed a unified diffusion-based framework for low-level vision tasks such as colorization, inpainting, cropping, and restoration. With its simple and general idea, this work demonstrated the superior performance of diffusion models compared to GAN models. DiffC [193] proposed an unconditional generative approach that encoded and denoised corrupted pixels with a single diffusion model, which showed the potential of diffusion models in lossy image compression. SRDiff [28] exploited the diffusion-based single-image super-resolution model and showed competitive results. RePaint [194] was a free-form inpainting method that directly employed a pre-trained diffusion model as the generative prior and only replaced the reverse diffusion by sampling the unmasked regions using the given image information. Though there was no modification to the vanilla pre-trained diffusion model, this method was able to outperform autoregressive and GAN methods under extreme tasks.

4.1.2 High-level vision

FSDM [29] was a few-shot generation framework based on conditional diffusion models. Leveraging advances in vision transformers and diffusion models, FSDM can adapt quickly to various generative processes at test-time and performs well under few-shot generation with strong transfer capability. CARD [30] proposed classification and regression diffusion models, combining a denoising diffusion-based conditional generative model and a pre-trained conditional mean estimator to predict data distribution under given conditions. Though approaching supervised learning from a conditional generation perspective and training with objectives indirectly related to the evaluation metrics, CARD presented a strong ability in uncertainty estimation with the help of diffusion models. Motivated by CLIP [195], GLIDE [171] explored realistic image synthesis conditioned on the text and found that diffusion models with classifier-free guidance yielded high-quality images containing a wide range of learned knowledge. DreamFusion [196] extends GLIDE's achievement into 3D space. To obtain expressive generative models within a smooth and limited space, LSGM [101] built a diffusion model trained in the latent space with the help of a variational autoencoder framework. SegDiff [197] extended diffusion models for performing image-level segmentation by summing up feature maps from a diffusion-based probabilistic encoder and an image feature encoder. Video diffusion [198], on the other hand, extended diffusion models in the time axis and performed video-level generation by utilizing a typically designed reconstruction-guided conditional sampling method. VQ-Diffusion [31] improved vanilla vector quantized diffusion by exploring classifier-free guidance sampling for discrete diffusion models and presenting a high-quality inference strategy. This method showed superior performance on large datasets such as ImageNet [199] and MSCOCO [200]. Diff-SCM [201] built a deep structural model based on the generative diffusion model. It achieved counterfactual estimation by inferring latent variables with deterministic forward diffusion and intervening in the backward process.

4.1.3 3D vision

[32] was an early work on diffusion-based 3D vision tasks. Motivated by the non-equilibrium thermodynamics, this work analogized points in point clouds as particles in a thermodynamic system and employed the diffusion process in point cloud generation, which achieved competitive performance. PVD [202] was a concurrent work on diffusion-based point cloud generation but performed unconditional generation without additional shape encoders, while a hybrid and point-voxel representation was employed for processing shapes. PDR [33] proposed a paradigm for diffusion-based point cloud completion that applied a diffusion model to generate a coarse completion based on the partial observation and refined the generated output by another network. To deal with point cloud denoising, [34] introduced a neural network to estimate the score of the distribution and denoised point clouds by gradient ascent.

4.1.4 Video modeling

Video diffusion [198] introduced the advances in diffusion-based generative models into the video domain. RVD [203]

employed diffusion models to generate a residual to a deterministic next-frame prediction conditioned on the context vector. FDM [204] applied diffusion models to assist long video prediction and performed photo-realistic videos. MCVD [35] proposed a conditional video diffusion framework for video prediction and interpolation based on masking frames in a blockwise manner. RaMViD [36] extended image diffusion models to videos with 3D convolutional neural networks and designed a conditioning technique for video prediction, infilling, and upsampling.

4.1.5 Medical application

It is a natural choice to apply diffusion models to medical images. Score-MRI [37] proposed a diffusion-based framework to solve magnetic resonance imaging (MRI) reconstruction. [205] was a concurrent work but provided a more flexible framework that did not require a paired dataset for training. With a diffusion model trained on medical images, this work leveraged the physical measurement process and focused on sampling algorithms to create image samples that are consistent with the observed measurements and the estimated data prior. R2D2+ [206] combined diffusion-based MRI reconstruction and super-resolution into the same network for end-to-end high-quality medical image generation. [207] explored the application of the generative diffusion model to medical image segmentation and performed counterfactual diffusion.

4.2 Sequential modeling

4.2.1 Natural language processing

Benefited by the non-autoregressive mechanism of diffusion models, Diffusion-LM [38] took advantage of continuous diffusions to iteratively denoise noisy vectors into word vectors and performed controllable text generation tasks. Bit Diffusion [39] proposed a diffusion model for generating discrete data and was applied to image caption tasks.

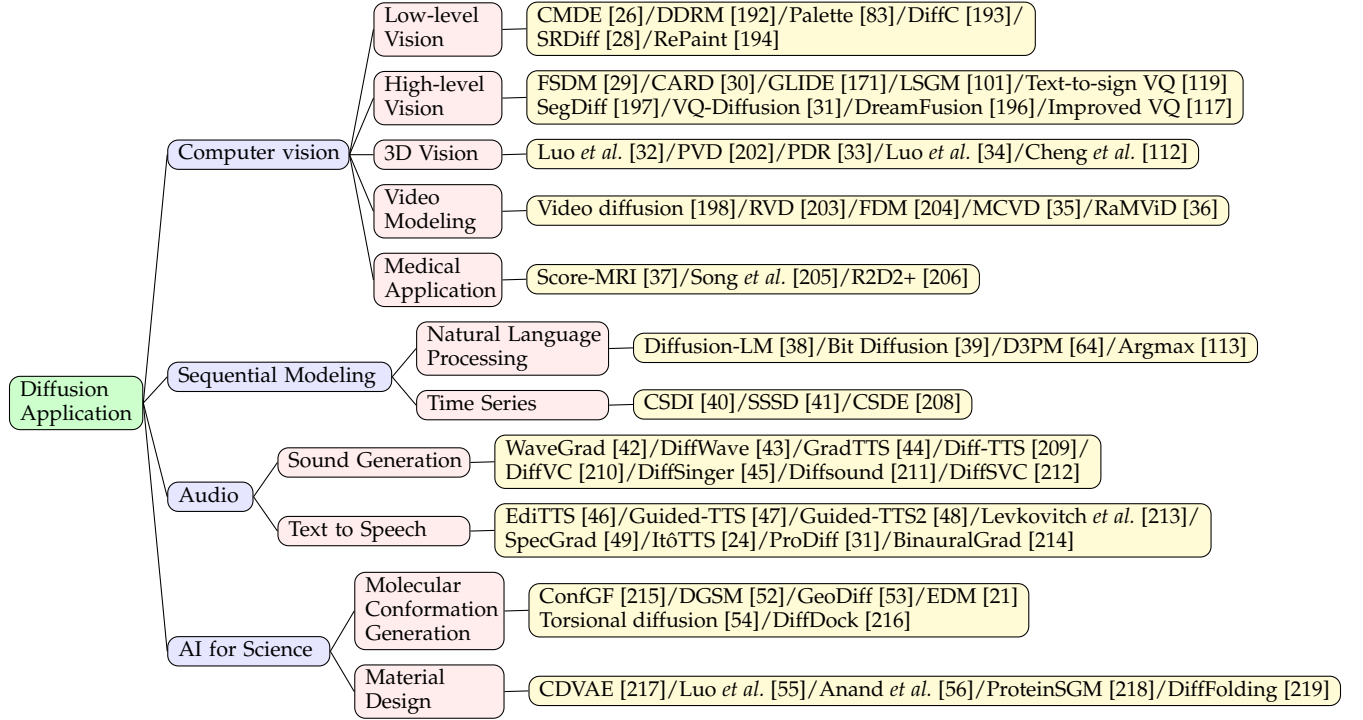
4.2.2 Time series

To deal with time series imputation, CSDI [40] utilized score-based diffusion models conditioned on observed data. Inspired by masked language modeling, a self-supervised training procedure was developed that separates observed values into conditional information and imputation targets. SSSD [41] further introduced structured state space models to capture long-term dependencies in time series data. CSDE [208] proposed a probabilistic framework to model stochastic dynamics and introduced Markov dynamic programming and multi-conditional forward-backward losses to generate complex time series.

4.3 Audio

WaveGrad [42] and DiffWave [43] were seminal works that applied diffusion models to raw waveform generation and obtained superior performance. GradTTS [44] and DiffTTS [209] also implemented diffusion models but generated mel feature instead of raw waves. DiffVC [210] further challenged the one-shot many-to-many voice conversion problem and developed a stochastic differential equation solver. DiffSinger [45] extended the common sound generation to singing voice synthesis based on a shallow diffusion

TABLE 3
Classification of Diffusion-based model Applications



mechanism. Diffsound [211] proposed a sound generation framework conditioned on the text that employed a discrete diffusion model to replace the autoregressive decoder to overcome the unidirectional bias and accumulated errors. EdiTTS [46] was also a diffusion-based audio model for the text-to-speech task. Through coarse perturbations in the prior space, desired edits were induced during denoising reversal. Guided-TTS [47] and Guided-TTS2 [48] were also an early series of text-to-speech models that successfully applied diffusion models in sound generation. [213] combined a voice diffusion model with a spectrogram-domain conditioning method and performed text-to-speech with voices unseen during training. InferGrad [220] considered the inference process in training and improved the diffusion-based text-to-speech model when the number of inference steps is small, enabling fast and high-quality sampling. SpecGrad [49] brought ideas from signal processing and adapted the time-varying spectral envelope of diffusion noise based on the conditioning log-mel spectrogram. ItōTTS [24] unified text-to-speech and vocoder into a framework based on linear SDE. ProDiff [31] proposed a progressive and fast diffusion model for high-quality text-to-speech. Instead of hundreds of iterations, ProDiff parameterized the model by predicting clean data and employed a teacher-synthesized mel-spectrogram as a target to reduce data discrepancies and make a sharp prediction. Binaural-Grad [214] was a two-stage diffusion-based framework that explored the application of diffusion models in binaural audio synthesis given mono audio.

4.4 AI for science

4.4.1 Molecular conformation generation

ConfGF [215] was an early work on diffusion-based molecular conformation generation models. While preserving rotation and translation equivariance, ConfGF generated samples by Langevin dynamics with physically inspired gradient fields. However, ConfGF only modeled local distances between the first-order, the second-order, and the third-order neighbors and thus failed to capture long-range interactions between non-bounded atoms. To tackle this challenge, DGSM [52] proposed to dynamically construct molecular graph structures between atoms based on their spatial proximity. GeoDiff [53] found that the model was fed with perturbed distance matrices during diffusion learning, which might violate mathematical constraints. Thus, GeoDiff introduced a roto-translational invariant Markov process to impose constraints on the density. EDM [21] further extended the above methods by incorporating discrete atom features and deriving the equations required for log-likelihood computation. Torsional diffusion [54] operated on the space of torsional angles and produced molecular conformations according to a diffusion process limited to the most flexible degrees of freedom. Based on previous geometric deep learning methods, DiffDock [216] conducts denoised score matching on transition, rotation, and torsion angle to generate drug conformation in protein-ligand complexes.

4.4.2 Material design

CDVAE [217] explored the periodic structure of stable material generation. To address the challenge that stable materials exist only in a low-dimensional subspace with all pos-

sible periodic arrangements of atoms, CDVAE designed a diffusion-based network as a decoder with output gradients leading to local minima of energy and updated atom types to capture specific local bonding preferences depending on the neighbors.

Inspired by the recent success of antibody modeling [221], [222], [223], the recent work [55] developed a diffusion-based generative model that explicitly targeted specific antigen structures and generated antibodies. The proposed method jointly sampled antibody sequences and structures and iteratively generated candidates in the sequence-structure space.

Anand *et al.* [56] introduced a diffusion-based generative model for both protein structure and sequence and learned the structural information that is equivariant to rotations and translations. ProteinSGM [218] formulated protein design as an image inpainting problem and applied conditional diffusion-based generation to precisely model the protein structure. DiffFolding [219] generates protein backbone concentrating on internal angles by traditional DDPM idea.

5 CONCLUSIONS & DISCUSSIONS

The diffusion model becomes increasingly crucial to a wide range of applied fields. To utilize the power of the diffusion model, this paper provides a comprehensive and up-to-date review of several aspects of diffusion models using detailed insights on various attitudes, including theory, improved algorithms, and applications. We hope this survey serves as a guide for readers on diffusion model enhancement and its application.

6 LIMITATIONS & FURTHER DIRECTIONS

Attention on diffusion model class: Most existing improvements and application algorithms are based on the original setting as DDPM. However, many aspects are ignored by researchers concerning the generalized setting of diffusion-based models. What if the prior distribution comes into any random distribution? Can the original data be rebuilt? What if the perturbation kernels are changed into Bernoulli distribution? Does it make sense in some specific circumstances? How slight the perturbation is suitable for the diffusion process? How many steps are enough for data generation? Thus, further meaningful works that explore prior distribution, transition kernel, sampling algorithm, and diffusion schemes are expected. Diffusion models should be viewed as a class, but not a branch of DDPM-based models.

Training objective & evaluation metric: Most diffusion-based models set training objectives as evidence of lower bound (ELBO) of negative log-likelihood. However, we have no clear theory that ELBO and NLL are optimized simultaneously. Therefore, the inconsistency may lead to a hidden mismatch between the real goal and the practical refinement of designing. Consequently, further analytical approaches linking log-likelihood optimization to existing variables or creating novel training objectives consistent with the likelihood may guide a significant enhancement of the model's performance. Furthermore, current evaluation

metrics like FID and IS scores cannot perfectly match the primary goals since data distributions are not equivariant to likelihood matching. The ideal evaluation metric should test the sample diversity as well as the recovery effect of diffusion models. A diversity score considering enough classes like CLIP [195] may be an available solution. A recovery score considering real-world data on the manifold for distribution distance will describe the model's generating ability more accurately and comprehensively. To sum up, the training objective and evaluation metric need to follow the initial goal.

Application and inductive bias: Various fields such as AI for science and natural language processing achieve significant progress with the aid of generative models but require complex modeling to eliminate the inductive bias. There is a range of tasks that still require refinement with diffusion models to obtain better performance than existing generative networks. For current tasks based on diffusion models, the corresponding frameworks are dominated by score-based networks and DDPM. Accordingly, improvement algorithms with reduced steps should draw much attention, which is one of our motivations for this survey.

ACKNOWLEDGMENTS

This work is supported by the Science and Technology Innovation 2030 - Major Project (No. 2021ZD0150100) and the National Natural Science Foundation of China (No. U21A20427).

We appreciate Dr. Jindong Wang provided the idea for our classification figures.

REFERENCES

- [1] D. J. Rezende, S. Mohamed, and D. Wierstra, "Stochastic back-propagation and approximate inference in deep generative models," in *International conference on machine learning*. PMLR, 2014, pp. 1278–1286. (document)
- [2] C. Doersch, "Tutorial on variational autoencoders," *arXiv preprint arXiv:1606.05908*, 2016. (document)
- [3] D. P. Kingma, M. Welling *et al.*, "An introduction to variational autoencoders," *Foundations and Trends® in Machine Learning*, vol. 12, no. 4, pp. 307–392, 2019. (document)
- [4] A. Oussidi and A. Elhassouny, "Deep generative models: Survey," in *2018 International Conference on Intelligent Systems and Computer Vision (ISCV)*. IEEE, 2018, pp. 1–8. (document)
- [5] Y. LeCun, S. Chopra, R. Hadsell, M. Ranzato, and F. Huang, "A tutorial on energy-based learning," *Predicting structured data*, vol. 1, no. 0, 2006. (document)
- [6] J. Ngiam, Z. Chen, P. W. Koh, and A. Y. Ng, "Learning deep energy models," in *Proceedings of the 28th international conference on machine learning (ICML-11)*, 2011, pp. 1105–1112. (document)
- [7] A. G. ALIAS PARTH GOYAL, N. R. Ke, S. Ganguli, and Y. Bengio, "Variational walkback: Learning a transition operator as a stochastic recurrent net," *Advances in Neural Information Processing Systems*, vol. 30, 2017. (document)
- [8] T. Kim and Y. Bengio, "Deep directed generative models with energy-based probability estimation," *arXiv preprint arXiv:1606.03439*, 2016. (document)
- [9] I. Goodfellow, J. Pouget-Abadie, M. Mirza, B. Xu, D. Warde-Farley, S. Ozair, A. Courville, and Y. Bengio, "Generative adversarial networks," *Communications of the ACM*, vol. 63, no. 11, pp. 139–144, 2020. (document)
- [10] A. Creswell, T. White, V. Dumoulin, K. Arulkumaran, B. Gupta, and A. A. Bharath, "Generative adversarial networks: An overview," *IEEE signal processing magazine*, vol. 35, no. 1, pp. 53–65, 2018. (document)

[11] J. Gui, Z. Sun, Y. Wen, D. Tao, and J. Ye, "A review on generative adversarial networks: Algorithms, theory, and applications," *IEEE Transactions on Knowledge and Data Engineering*, 2021. (document)

[12] M. Mirza and S. Osindero, "Conditional generative adversarial nets," *arXiv preprint arXiv:1411.1784*, 2014. (document)

[13] M. Arjovsky, S. Chintala, and L. Bottou, "Wasserstein generative adversarial networks," in *International conference on machine learning*. PMLR, 2017, pp. 214–223. (document)

[14] L. Dinh, J. Sohl-Dickstein, and S. Bengio, "Density estimation using real nvp," *arXiv preprint arXiv:1605.08803*, 2016. (document)

[15] D. Rezende and S. Mohamed, "Variational inference with normalizing flows," in *International conference on machine learning*. PMLR, 2015, pp. 1530–1538. (document)

[16] I. Kobyzev, S. J. Prince, and M. A. Brubaker, "Normalizing flows: An introduction and review of current methods," *IEEE transactions on pattern analysis and machine intelligence*, vol. 43, no. 11, pp. 3964–3979, 2020. (document)

[17] S. Bond-Taylor, A. Leach, Y. Long, and C. Willcocks, "Deep generative modelling: A comparative review of vaes, gans, normalizing flows, energy-based and autoregressive models." *IEEE Transactions on Pattern Analysis and Machine Intelligence*, 2021. (document)

[18] G. Papamakarios, E. T. Nalisnick, D. J. Rezende, S. Mohamed, and B. Lakshminarayanan, "Normalizing flows for probabilistic modeling and inference." *J. Mach. Learn. Res.*, vol. 22, no. 57, pp. 1–64, 2021. (document), 1

[19] C. Winkler, D. Worrall, E. Hoogeboom, and M. Welling, "Learning likelihoods with conditional normalizing flows," *arXiv preprint arXiv:1912.00042*, 2019. (document)

[20] C. Saharia, W. Chan, H. Chang, C. A. Lee, J. Ho, T. Salimans, D. J. Fleet, and M. Norouzi, "Palette: Image-to-image diffusion models," 2021. [Online]. Available: <https://arxiv.org/abs/2111.05826> (document)

[21] E. Hoogeboom, V. G. Satorras, C. Vignac, and M. Welling, "Equivariant diffusion for molecule generation in 3d," in *International Conference on Machine Learning*. PMLR, 2022, pp. 8867–8887. (document), 3.2.1, 3, 4.4.1, 9

[22] S. Luo, Y. Su, X. Peng, S. Wang, J. Peng, and J. Ma, "Antigen-specific antibody design and optimization with diffusion-based generative models," *bioRxiv*, 2022. [Online]. Available: <https://www.biorxiv.org/content/early/2022/07/11/2022.07.10.499510> (document), 3.2.1

[23] H. Tachibana, M. Go, M. Inahara, Y. Katayama, and Y. Watanabe, "It^o-taylor sampling scheme for denoising diffusion probabilistic models using ideal derivatives," *arXiv preprint arXiv:2112.13339*, 2021. (document), 2, 3.1.2, 8

[24] S. Wu and Z. Shi, "Itôts and itôwave: Linear stochastic differential equation is all you need for audio generation," *arXiv e-prints*, pp. arXiv–2105, 2021. (document), 3, 4.3, 9

[25] J. Sohl-Dickstein, E. Weiss, N. Maheswaranathan, and S. Ganguli, "Deep unsupervised learning using nonequilibrium thermodynamics," in *International Conference on Machine Learning*. PMLR, 2015, pp. 2256–2265. (document), 2.1.4, 8

[26] G. Batzolos, J. Stanczuk, C.-B. Schönlieb, and C. Ettrmann, "Conditional image generation with score-based diffusion models," *arXiv preprint arXiv:2111.13606*, 2021. (document), 4.1.1, 3, 9

[27] L. Theis, A. van den Oord, and M. Bethge, "A note on the evaluation of generative models," in *International Conference on Learning Representations (ICLR 2016)*, 2016, pp. 1–10. (document), 3.2.1

[28] H. Li, Y. Yang, M. Chang, S. Chen, H. Feng, Z. Xu, Q. Li, and Y. Chen, "Srdiff: Single image super-resolution with diffusion probabilistic models," *Neurocomputing*, vol. 479, pp. 47–59, 2022. (document), 4.1.1, 3, 9

[29] G. Giannone, D. Nielsen, and O. Winther, "Few-shot diffusion models," *arXiv preprint arXiv:2205.15463*, 2022. (document), 4.1.2, 3, 9

[30] X. Han, H. Zheng, and M. Zhou, "Card: Classification and regression diffusion models," *arXiv preprint arXiv:2206.07275*, 2022. (document), 4.1.2, 3, 9

[31] R. Huang, Z. Zhao, H. Liu, J. Liu, C. Cui, and Y. Ren, "Prodiff: Progressive fast diffusion model for high-quality text-to-speech," *arXiv preprint arXiv:2207.06389*, 2022. (document), 4.1.2, 3, 4.3, 9

[32] S. Luo and W. Hu, "Diffusion probabilistic models for 3d point cloud generation," in *Proceedings of the IEEE/CVF Conference on Computer Vision and Pattern Recognition*, 2021, pp. 2837–2845. (document), 2, 3.2.1, 4.1.3, 3, 8, 9

[33] Z. Lyu, Z. Kong, X. Xu, L. Pan, and D. Lin, "A conditional point diffusion-refinement paradigm for 3d point cloud completion," *arXiv preprint arXiv:2112.03530*, 2021. (document), 2, 3.2.1, 4.1.3, 3, 8, 9

[34] S. Luo and W. Hu, "Score-based point cloud denoising," in *Proceedings of the IEEE/CVF International Conference on Computer Vision*, 2021, pp. 4583–4592. (document), 4.1.3, 3, 9

[35] V. Voleti, A. Jolicoeur-Martineau, and C. Pal, "Mcvd: Masked conditional video diffusion for prediction, generation, and interpolation," *arXiv preprint arXiv:2205.09853*, 2022. (document), 4.1.4, 3, 9

[36] T. Höppe, A. Mehrjou, S. Bauer, D. Nielsen, and A. Dittadi, "Diffusion models for video prediction and infilling," *arXiv preprint arXiv:2206.07696*, 2022. (document), 4.1.4, 3, 9

[37] H. Chung and J. C. Ye, "Score-based diffusion models for accelerated mri," *Medical Image Analysis*, p. 102479, 2022. (document), 4.1.5, 3, 9

[38] X. L. Li, J. Thickstun, I. Gulrajani, P. Liang, and T. B. Hashimoto, "Diffusion-lm improves controllable text generation," *arXiv preprint arXiv:2205.14217*, 2022. (document), 4.2.1, 3, 9

[39] T. Chen, R. Zhang, and G. Hinton, "Analog bits: Generating discrete data using diffusion models with self-conditioning," *arXiv preprint arXiv:2208.04202*, 2022. (document), 4.2.1, 3, 9

[40] Y. Tashiro, J. Song, Y. Song, and S. Ermon, "Csdi: Conditional score-based diffusion models for probabilistic time series imputation," *Advances in Neural Information Processing Systems*, vol. 34, pp. 24804–24816, 2021. (document), 4.2.2, 3, 9

[41] J. M. L. Alcaraz and N. Strodthoff, "Diffusion-based time series imputation and forecasting with structured state space models," *arXiv preprint arXiv:2208.09399*, 2022. (document), 4.2.2, 3, 9

[42] N. Chen, Y. Zhang, H. Zen, R. J. Weiss, M. Norouzi, and W. Chan, "Wavegrad: Estimating gradients for waveform generation," in *International Conference on Learning Representations*, 2020. (document), 3, 4.3, 3, 9

[43] Z. Kong, W. Ping, J. Huang, K. Zhao, and B. Catanzaro, "Diffwave: A versatile diffusion model for audio synthesis," in *International Conference on Learning Representations*, 2020. (document), 4.3, 3, 9

[44] V. Popov, I. Vovk, V. Gogoryan, T. Sadekova, and M. Kudinov, "Grad-tts: A diffusion probabilistic model for text-to-speech," in *International Conference on Machine Learning*. PMLR, 2021, pp. 8599–8608. (document), 4.3, 3, 9

[45] J. Liu, C. Li, Y. Ren, F. Chen, and Z. Zhao, "Diffsinger: Singing voice synthesis via shallow diffusion mechanism," in *Proceedings of the AAAI Conference on Artificial Intelligence*, vol. 36, no. 10, 2022, pp. 11020–11028. (document), 4.3, 3, 9

[46] J. Tae, H. Kim, and T. Kim, "Edits: Score-based editing for controllable text-to-speech," *arXiv preprint arXiv:2110.02584*, 2021. (document), 3, 4.3, 9

[47] H. Kim, S. Kim, and S. Yoon, "Guided-tts: A diffusion model for text-to-speech via classifier guidance," in *International Conference on Machine Learning*. PMLR, 2022, pp. 11119–11133. (document), 3.2, 3, 4.3, 9

[48] S. Kim, H. Kim, and S. Yoon, "Guided-tts 2: A diffusion model for high-quality adaptive text-to-speech with untranscribed data," *arXiv preprint arXiv:2205.15370*, 2022. (document), 3, 4.3, 9

[49] Y. Koizumi, H. Zen, K. Yatabe, N. Chen, and M. Bacchiani, "Specgrad: Diffusion probabilistic model based neural vocoder with adaptive noise spectral shaping," *arXiv preprint arXiv:2203.16749*, 2022. (document), 3, 4.3, 9

[50] Z. Kong, W. Ping, J. Huang, K. Zhao, and B. Catanzaro, "Diffwave: A versatile diffusion model for audio synthesis," 2020. [Online]. Available: <https://arxiv.org/abs/2009.09761> (document)

[51] H. Kim, S. Kim, and S. Yoon, "Guided-tts: A diffusion model for text-to-speech via classifier guidance," 2021. [Online]. Available: <https://arxiv.org/abs/2111.11755> (document)

[52] S. Luo, C. Shi, M. Xu, and J. Tang, "Predicting molecular conformation via dynamic graph score matching," *Advances in Neural Information Processing Systems*, vol. 34, pp. 19784–19795, 2021. (document), 3, 4.4.1, 9

[53] M. Xu, L. Yu, Y. Song, C. Shi, S. Ermon, and J. Tang, "Geodiff: A geometric diffusion model for molecular conformation generation," in *International Conference on Learning Representations*, 2021. (document), 3, 4.4.1, 9

[54] B. Jing, G. Corso, R. Barzilay, and T. S. Jaakkola, "Torsional diffusion for molecular conformer generation," in *ICLR2022 Machine Learning for Drug Discovery*, 2022. (document), 3.2, 3, 4.4.1, 9

[55] S. Luo, Y. Su, X. Peng, S. Wang, J. Peng, and J. Ma, "Antigen-specific antibody design and optimization with diffusion-based generative models," *bioRxiv*, 2022. (document), 3.2, 3, 4.4.2, 9

[56] N. Anand and T. Achim, "Protein structure and sequence generation with equivariant denoising diffusion probabilistic models," *arXiv preprint arXiv:2205.15019*, 2022. (document), 3, 4.4.2, 9

[57] I. J. Goodfellow, J. Pouget-Abadie, M. Mirza, B. Xu, D. Warde-Farley, S. Ozair, A. Courville, and Y. Bengio, "Generative adversarial networks," 2014. [Online]. Available: <https://arxiv.org/abs/1406.2661> 1

[58] I. Goodfellow, Y. Bengio, and A. Courville, *Deep Learning*. MIT Press, 2016, <http://www.deeplearningbook.org>. 1

[59] D. P. Kingma and M. Welling, "Auto-encoding variational bayes," *arXiv preprint arXiv:1312.6114*, 2013. 1

[60] A. Q. Nichol and P. Dhariwal, "Improved denoising diffusion probabilistic models," in *International Conference on Machine Learning*. PMLR, 2021, pp. 8162–8171. (document), 2, 3.1.1, 3.3, 3.3.1, B.3, 6, 7, 8

[61] T. Salimans and J. Ho, "Progressive distillation for fast sampling of diffusion models," *arXiv preprint arXiv:2202.00512*, 2022. (document), 3, 2, 3.1.1, 7, 8

[62] Z. Xiao, K. Kreis, and A. Vahdat, "Tackling the generative learning trilemma with denoising diffusion gans," *arXiv preprint arXiv:2112.07804*, 2021. (document), 2, 3.1.3, 7, 8

[63] C. Lu, Y. Zhou, F. Bao, J. Chen, C. Li, and J. Zhu, "Dpm-solver: A fast ode solver for diffusion probabilistic model sampling in around 10 steps," 2022. [Online]. Available: <https://arxiv.org/abs/2206.00927> (document), 2.2.3, 2, 3.1.2, 4, 5, 7, 8

[64] J. Austin, D. D. Johnson, J. Ho, D. Tarlow, and R. van den Berg, "Structured denoising diffusion models in discrete state-spaces," *Advances in Neural Information Processing Systems*, vol. 34, pp. 17981–17993, 2021. (document), 2, 3.2.2, 3.3.1, 3, 6, 8, 9

[65] Y. Song, J. Sohl-Dickstein, D. P. Kingma, A. Kumar, S. Ermon, and B. Poole, "Score-based generative modeling through stochastic differential equations," *arXiv preprint arXiv:2011.13456*, 2020. 2.1.3, 2.2.3, 2.2.3, 2, 3.1.2, 3.1.4, 3.2.3, 6, 8

[66] D. Kingma, T. Salimans, B. Poole, and J. Ho, "Variational diffusion models," *Advances in neural information processing systems*, vol. 34, pp. 21696–21707, 2021. 2.1.3, 2, 3.1.1, 3.1.4, 3.3.1, 6, 8

[67] J. Ho, A. Jain, and P. Abbeel, "Denoising diffusion probabilistic models," *Advances in Neural Information Processing Systems*, vol. 33, pp. 6840–6851, 2020. 2.2, 2.2.1, 2.2.1, 2.2.1, 3.3, 6, 8

[68] J. Song, C. Meng, and S. Ermon, "Denoising diffusion implicit models," in *International Conference on Learning Representations*, 2020. 2.2, 2, 3.1.2, 7, 8

[69] Y. Song and S. Ermon, "Generative modeling by estimating gradients of the data distribution," *Advances in Neural Information Processing Systems*, vol. 32, 2019. 2.2.2, 2.3.2, 4.1.1, 4, 6, 8

[70] S. Lyu, "Interpretation and generalization of score matching," *arXiv preprint arXiv:1205.2629*, 2012. 2.2.2

[71] L. Arnold, "Stochastic differential equations," *New York*, 1974. 2.2.3

[72] B. Oksendal, *Stochastic differential equations: an introduction with applications*. Springer Science & Business Media, 2013. 2.2.3

[73] A. Hyvärinen and P. Dayan, "Estimation of non-normalized statistical models by score matching," *Journal of Machine Learning Research*, vol. 6, no. 4, 2005. 2.2.3, 2.3.2

[74] D. Maoutsu, S. Reich, and M. Opper, "Interacting particle solutions of fokker-planck equations through gradient-log-density estimation," *Entropy*, vol. 22, no. 8, p. 802, 2020. 2.2.3

[75] R. T. Chen, Y. Rubanova, J. Bettencourt, and D. K. Duvenaud, "Neural ordinary differential equations," *Advances in neural information processing systems*, vol. 31, 2018. 2.2.3, 3.1.2, 3.1.2, 3.1.4

[76] L. Liu, Y. Ren, Z. Lin, and Z. Zhao, "Pseudo numerical methods for diffusion models on manifolds," *arXiv preprint arXiv:2202.09778*, 2022. 2.2.3, 2, 3.1.2, 3.2.3, 4, 8

[77] Y. Song, S. Garg, J. Shi, and S. Ermon, "Sliced score matching: A scalable approach to density and score estimation," in *Uncertainty in Artificial Intelligence*. PMLR, 2020, pp. 574–584. 2.3.2, 6

[78] R. M. Neal, "Annealed importance sampling," *Statistics and computing*, vol. 11, no. 2, pp. 125–139, 2001. 2.4.1

[79] R. W. Hamming, "Stable predictor-corrector methods for ordinary differential equations," *Journal of the ACM (JACM)*, vol. 6, no. 1, pp. 37–47, 1959. 2.4.3

[80] J. R. Dormand and P. J. Prince, "A family of embedded runge-kutta formulae," *Journal of computational and applied mathematics*, vol. 6, no. 1, pp. 19–26, 1980. 2.4.3

[81] T. Sauer, *Numerical analysis*. Addison-Wesley Publishing Company, 2011. 2.4.3

[82] W. H. Press, S. A. Teukolsky, W. T. Vetterling, and B. P. Flannery, *Numerical recipes 3rd edition: The art of scientific computing*. Cambridge university press, 2007. 2.4.3

[83] C. Saharia, W. Chan, H. Chang, C. Lee, J. Ho, T. Salimans, D. Fleet, and M. Norouzi, "Palette: Image-to-image diffusion models," in *ACM SIGGRAPH 2022 Conference Proceedings*, 2022, pp. 1–10. 3, 4.1.1, 3, 9

[84] E. Luhman and T. Luhman, "Knowledge distillation in iterative generative models for improved sampling speed," *arXiv preprint arXiv:2101.02388*, 2021. 2, 7, 8

[85] H. Zheng, P. He, W. Chen, and M. Zhou, "Truncated diffusion probabilistic models," *arXiv preprint arXiv:2202.09671*, 2022. 2, 3.1.1, 6, 7, 8

[86] Z. Lyu, X. Xu, C. Yang, D. Lin, and B. Dai, "Accelerating diffusion models via early stop of the diffusion process," *arXiv preprint arXiv:2205.12524*, 2022. 2, 3.1.1, 3.1.3, 4, 5, 7, 8

[87] H. Chung, B. Sim, and J. C. Ye, "Come-closer-diffuse-faster: Accelerating conditional diffusion models for inverse problems through stochastic contraction," in *Proceedings of the IEEE/CVF Conference on Computer Vision and Pattern Recognition*, 2022, pp. 12413–12422. 2, 3.1.1, 8

[88] G. Franzese, S. Rossi, L. Yang, A. Finamore, D. Rossi, M. Filippone, and P. Michiardi, "How much is enough? a study on diffusion times in score-based generative models," 2022. [Online]. Available: <https://arxiv.org/abs/2206.05173> 2, 3.1.1, 7, 8

[89] Z. Kong and W. Ping, "On fast sampling of diffusion probabilistic models," *arXiv preprint arXiv:2106.00132*, 2021. 2, 3.1.1, 3.1.2, 3.1.4, 7, 8

[90] R. San-Roman, E. Nachmani, and L. Wolf, "Noise estimation for generative diffusion models," *arXiv preprint arXiv:2104.02600*, 2021. 2, 8

[91] F. Bao, C. Li, J. Zhu, and B. Zhang, "Analytic-dpm: an analytic estimate of the optimal reverse variance in diffusion probabilistic models," *arXiv preprint arXiv:2201.06503*, 2022. 2, 3.1.2, 4, 5, 6, 7, 8

[92] F. Bao, C. Li, J. Sun, J. Zhu, and B. Zhang, "Estimating the optimal covariance with imperfect mean in diffusion probabilistic models," *arXiv preprint arXiv:2206.07309*, 2022. 2, 3.1.2, 4, 5, 6, 7, 8

[93] Q. Zhang and Y. Chen, "Fast sampling of diffusion models with exponential integrator," *arXiv preprint arXiv:2204.13902*, 2022. 2, 3.1.2, 6, 7, 8

[94] Q. Zhang, M. Tao, and Y. Chen, "gddim: Generalized denoising diffusion implicit models," *arXiv preprint arXiv:2206.05564*, 2022. 2, 3.1.2, 3.1.4, 7, 8

[95] D. Watson, J. Ho, M. Norouzi, and W. Chan, "Learning to efficiently sample from diffusion probabilistic models," *arXiv preprint arXiv:2106.03802*, 2021. 2, 3.1.2, 3.1.4, 5, 8

[96] T. Karras, M. Aittala, T. Aila, and S. Laine, "Elucidating the design space of diffusion-based generative models," *arXiv preprint arXiv:2206.00364*, 2022. 2, 3.1.2, 7, 8

[97] A. Jolicoeur-Martineau, K. Li, R. Piché-Taillefer, T. Kachman, and I. Mitliagkas, "Gotta go fast when generating data with score-based models," 2021. [Online]. Available: <https://arxiv.org/abs/2105.14080> 2, 3.1.2, 6, 7

[98] D. Watson, W. Chan, J. Ho, and M. Norouzi, "Learning fast samplers for diffusion models by differentiating through sample quality," 2, 3.1.2, 5, 7, 8

[99] K. Pandey, A. Mukherjee, P. Rai, and A. Kumar, "Diffusevae: Efficient, controllable and high-fidelity generation from low-dimensional latents," 2022. [Online]. Available: <https://arxiv.org/abs/2201.00308> 2, 3.1.3, 4, 6, 7, 8

[100] Q. Zhang and Y. Chen, "Diffusion normalizing flow," *Advances in Neural Information Processing Systems*, vol. 34, pp. 16280–16291, 2021. 2, 3.1.3, 7, 8

[101] A. Vahdat, K. Kreis, and J. Kautz, "Score-based generative modeling in latent space," *Advances in Neural Information Processing*

Systems, vol. 34, pp. 11287–11302, 2021. 2, 3.1.3, 3.4, 4.1.2, 3, 7, 8, 9

[102] Y. Song, C. Durkan, I. Murray, and S. Ermon, “Maximum likelihood training of score-based diffusion models,” *Advances in Neural Information Processing Systems*, vol. 34, pp. 1415–1428, 2021. 2, 3.1.3, 3.2.1, 3.3, 3.3.1, 8

[103] D. Kim, B. Na, S. J. Kwon, D. Lee, W. Kang, and I.-c. Moon, “Maximum likelihood training of parametrized diffusion model,” 2021. 2, 3.1.3, 3.3.2, 3.4, 8

[104] D. Kim, B. Na, S. J. Kwon, D. Lee, W. Kang, and I.-c. Moon, “Maximum likelihood training of implicit nonlinear diffusion models,” *arXiv preprint arXiv:2205.13699*, 2022. 2, 3.4, 6, 8

[105] R. Gao, Y. Song, B. Poole, Y. N. Wu, and D. P. Kingma, “Learning energy-based models by diffusion recovery likelihood,” *arXiv preprint arXiv:2012.08125*, 2020. 2, 3.1.3, 8

[106] Y. Song and D. P. Kingma, “How to train your energy-based models,” 2021. [Online]. Available: <https://arxiv.org/abs/2101.03288> 2, 8

[107] A. Bansal, E. Borgnia, H.-M. Chu, J. S. Li, H. Kazemi, F. Huang, M. Goldblum, J. Geiping, and T. Goldstein, “Cold diffusion: Inverting arbitrary image transforms without noise,” *arXiv preprint arXiv:2208.09392*, 2022. 2, 3.1.4, 3.2.1

[108] W. Gong and Y. Li, “Interpreting diffusion score matching using normalizing flow,” 2021. [Online]. Available: <https://arxiv.org/abs/2107.10072> 2, 3.1.4

[109] V. De Bortoli, A. Doucet, J. Heng, and J. Thornton, “Simulating diffusion bridges with score matching,” 2021. [Online]. Available: <https://arxiv.org/abs/2111.07243> 2, 3.1.4, 8

[110] C.-W. Huang, J. H. Lim, and A. C. Courville, “A variational perspective on diffusion-based generative models and score matching,” *Advances in Neural Information Processing Systems*, vol. 34, pp. 22863–22876, 2021. 2, 3.1.4, 3.3.1, 8

[111] L. Zhou, Y. Du, and J. Wu, “3d shape generation and completion through point-voxel diffusion,” in *Proceedings of the IEEE/CVF International Conference on Computer Vision (ICCV)*, October 2021, pp. 5826–5835. 2, 3.2.1, 8

[112] A.-C. Cheng, X. Li, S. Liu, M. Sun, and M.-H. Yang, “Autoregressive 3d shape generation via canonical mapping,” 2022. [Online]. Available: <https://arxiv.org/abs/2204.01955> 2, 3.2.1, 3, 9

[113] E. Hoogeboom, D. Nielsen, P. Jaini, P. Forré, and M. Welling, “Argmax flows and multinomial diffusion: Towards non-autoregressive language models,” 2021. 2, 3.2.2, 3, 8, 9

[114] E. Hoogeboom, A. A. Gritsenko, J. Bastings, B. Poole, R. v. d. Berg, and T. Salimans, “Autoregressive diffusion models,” *arXiv preprint arXiv:2110.02037*, 2021. 2, 3.2.2, 8

[115] A. Campbell, J. Benton, V. De Bortoli, T. Rainforth, G. Deligiannidis, and A. Doucet, “A continuous time framework for discrete denoising models,” *arXiv preprint arXiv:2205.14987*, 2022. 2, 8

[116] S. Gu, D. Chen, J. Bao, F. Wen, B. Zhang, D. Chen, L. Yuan, and B. Guo, “Vector quantized diffusion model for text-to-image synthesis,” in *Proceedings of the IEEE/CVF Conference on Computer Vision and Pattern Recognition*, 2022, pp. 10696–10706. 2, 3.2.2, 8, 9

[117] Z. Tang, S. Gu, J. Bao, D. Chen, and F. Wen, “Improved vector quantized diffusion models,” *arXiv preprint arXiv:2205.16007*, 2022. 2, 3.2.2, 3, 8, 9

[118] M. Cohen, G. Quispe, S. L. Corff, C. Ollion, and E. Moulines, “Diffusion bridges vector quantized variational autoencoders,” 2022. [Online]. Available: <https://arxiv.org/abs/2202.04895> 2, 3.2.2, 8

[119] P. Xie, Q. Zhang, Z. Li, H. Tang, Y. Du, and X. Hu, “Vector quantized diffusion model with codeunet for text-to-sign pose sequences generation,” 2022. [Online]. Available: <https://arxiv.org/abs/2208.09141> 2, 3.2.2, 3, 8, 9

[120] V. De Bortoli, E. Mathieu, M. Hutchinson, J. Thornton, Y. W. Teh, and A. Doucet, “Riemannian score-based generative modeling,” *arXiv preprint arXiv:2202.02763*, 2022. 2, 3.2.3, 8

[121] C.-W. Huang, M. Aghajohari, A. J. Bose, P. Panangaden, and A. Courville, “Riemannian diffusion models,” *arXiv preprint arXiv:2208.07949*, 2022. 2, 3.2.3, 8

[122] C. Niu, Y. Song, J. Song, S. Zhao, A. Grover, and S. Ermon, “Permutation invariant graph generation via score-based generative modeling,” in *International Conference on Artificial Intelligence and Statistics*. PMLR, 2020, pp. 4474–4484. 2, 3.2.3, 8

[123] D. Kim, S. Shin, K. Song, W. Kang, and I.-c. Moon, “Soft truncation: A universal training technique of score-based diffusion model for high precision score estimation,” 2021. [Online]. Available: <https://arxiv.org/abs/2106.05527> 2, 3.3.1, 4, 6, 8

[124] R. G. Lopes, S. Fenu, and T. Starner, “Data-free knowledge distillation for deep neural networks,” *arXiv preprint arXiv:1710.07535*, 2017. 3.1.1

[125] J. Gou, B. Yu, S. J. Maybank, and D. Tao, “Knowledge distillation: A survey,” *International Journal of Computer Vision*, vol. 129, no. 6, pp. 1789–1819, 2021. 3.1.1

[126] T. Choudhary, V. Mishra, A. Goswami, and J. Sarangapani, “A comprehensive survey on model compression and acceleration,” *Artificial Intelligence Review*, vol. 53, no. 7, pp. 5113–5155, 2020. 3.1.1

[127] Y. Cheng, D. Wang, P. Zhou, and T. Zhang, “A survey of model compression and acceleration for deep neural networks,” *arXiv preprint arXiv:1710.09282*, 2017. 3.1.1

[128] A. Polino, R. Pascanu, and D. Alistarh, “Model compression via distillation and quantization,” *arXiv preprint arXiv:1802.05668*, 2018. 3.1.1

[129] S. Sun, Y. Cheng, Z. Gan, and J. Liu, “Patient knowledge distillation for bert model compression,” in *Proceedings of the 2019 Conference on Empirical Methods in Natural Language Processing and the 9th International Joint Conference on Natural Language Processing (EMNLP-IJCNLP)*, 2019, pp. 4323–4332. 3.1.1

[130] R. Huang, Z. Zhao, H. Liu, J. Liu, C. Cui, and Y. Ren, “Prodiff: Progressive fast diffusion model for high-quality text-to-speech,” 2022. [Online]. Available: <https://arxiv.org/abs/2207.06389> 3.1.1

[131] H. Tsukamoto, S.-J. Chung, and J.-J. E. Slotine, “Contraction theory for nonlinear stability analysis and learning-based control: A tutorial overview,” *Annual Reviews in Control*, vol. 52, pp. 135–169, 2021. 3.1.1

[132] N. V. Hung, S. Migórski, V. M. Tam, and S. Zeng, “Gap functions and error bounds for variational–hemivariational inequalities,” *Acta Applicandae Mathematicae*, vol. 169, no. 1, pp. 691–709, 2020. 3.1.1

[133] H. Zheng and M. Zhou, “Act: Asymptotic conditional transport,” 2020. 3.1.1

[134] S. Mohamed and B. Lakshminarayanan, “Learning in implicit generative models,” *Learning*, no. 1/14, 2018. 3.1.2

[135] W. Grathwohl, R. T. Chen, J. Bettencourt, I. Sutskever, and D. Duvenaud, “Ffjord: Free-form continuous dynamics for scalable reversible generative models,” *arXiv preprint arXiv:1810.01367*, 2018. 3.1.2, 3.1.4

[136] Q. Han and S. Ji, “Novel multi-step predictor-corrector schemes for backward stochastic differential equations,” 2021. [Online]. Available: <https://arxiv.org/abs/2102.05915> 3.1.2

[137] T. Dockhorn, A. Vahdat, and K. Kreis, “Score-based generative modeling with critically-damped langevin diffusion,” *arXiv preprint arXiv:2112.07068*, 2021. 3.1.2

[138] M. Bayram, T. Partal, and G. Orucova Buyukoz, “Numerical methods for simulation of stochastic differential equations,” *Advances in Difference Equations*, vol. 2018, no. 1, pp. 1–10, 2018. 3.1.2

[139] V. F. Zaitsev and A. D. Polyanin, *Handbook of exact solutions for ordinary differential equations*. CRC press, 2002. 3.1.2

[140] E. Platen and N. Bruti-Liberati, *Numerical solution of stochastic differential equations with jumps in finance*. Springer Science & Business Media, 2010, vol. 64. 3.1.2

[141] E. Süli and D. F. Mayers, *An introduction to numerical analysis*. Cambridge university press, 2003. 3.1.2

[142] F. Rabiei, F. Ismail, and M. Suleiman, “Improved runge-kutta methods for solving ordinary differential equations,” *Sains Malaysiana*, vol. 42, no. 11, pp. 1679–1687, 2013. 3.1.2

[143] C. W. Gear and D. R. Wells, “Multirate linear multistep methods,” *BIT Numerical Mathematics*, vol. 24, no. 4, pp. 484–502, 1984. 3.1.2

[144] L. F. Shampine, *Numerical solution of ordinary differential equations*. Routledge, 2018. 3.1.2

[145] M. Hochbruck and A. Ostermann, “Exponential integrators,” *Acta Numerica*, vol. 19, pp. 209–286, 2010. 3.1.2

[146] T. H. Cormen, C. E. Leiserson, R. L. Rivest, and C. Stein, *Introduction to algorithms*. MIT press, 2022. 3.1.2

[147] R. Bellman, “The theory of dynamic programming,” *Bulletin of the American Mathematical Society*, vol. 60, no. 6, pp. 503–515, 1954. 3.1.2

[148] —, “Dynamic programming,” *Science*, vol. 153, no. 3731, pp. 34–37, 1966. 3.1.2

[149] R. E. Bellman and S. E. Dreyfus, *Applied dynamic programming*. Princeton university press, 2015, vol. 2050. 3.1.2

[150] D. Watson, W. Chan, J. Ho, and M. Norouzi, "Learning fast samplers for diffusion models by differentiating through sample quality," in *International Conference on Learning Representations*, 2021. 3.1.2

[151] R. Kumar, M. Purohit, Z. Svitkina, E. Vee, and J. Wang, "Efficient rematerialization for deep networks," *Advances in Neural Information Processing Systems*, vol. 32, 2019. 3.1.2

[152] R. Gao, X. Hou, J. Qin, J. Chen, L. Liu, F. Zhu, Z. Zhang, and L. Shao, "Zero-vae-gan: Generating unseen features for generalized and transductive zero-shot learning," *IEEE Transactions on Image Processing*, vol. 29, pp. 3665–3680, 2020. 3.1.3

[153] Z. Niu, K. Yu, and X. Wu, "Lstm-based vae-gan for time-series anomaly detection," *Sensors*, vol. 20, no. 13, p. 3738, 2020. 3.1.3

[154] A. Grover, M. Dhar, and S. Ermon, "Flow-gan: Combining maximum likelihood and adversarial learning in generative models," in *Proceedings of the AAAI conference on artificial intelligence*, vol. 32, no. 1, 2018. 3.1.3

[155] C. Ma and X. Zhang, "Gf-vae: A flow-based variational autoencoder for molecule generation," in *Proceedings of the 30th ACM International Conference on Information & Knowledge Management*, 2021, pp. 1181–1190. 3.1.3

[156] Z. Xiao, Q. Yan, and Y. Amit, "Generative latent flow," *arXiv preprint arXiv:1905.10485*, 2019. 3.1.3

[157] T. Han, E. Nijkamp, L. Zhou, B. Pang, S.-C. Zhu, and Y. N. Wu, "Joint training of variational auto-encoder and latent energy-based model," in *Proceedings of the IEEE/CVF Conference on Computer Vision and Pattern Recognition*, 2020, pp. 7978–7987. 3.1.3

[158] B. Pang, T. Han, E. Nijkamp, S.-C. Zhu, and Y. N. Wu, "Learning latent space energy-based prior model," *Advances in Neural Information Processing Systems*, vol. 33, pp. 21 994–22 008, 2020. 3.1.3

[159] J. Ho, X. Chen, A. Srinivas, Y. Duan, and P. Abbeel, "Flow++: Improving flow-based generative models with variational dequantization and architecture design," in *Proceedings of the 36th International Conference on Machine Learning*, ser. Proceedings of Machine Learning Research, K. Chaudhuri and R. Salakhutdinov, Eds., vol. 97. PMLR, 09–15 Jun 2019, pp. 2722–2730. [Online]. Available: <https://proceedings.mlr.press/v97/ho19a.html> 3.1.3, 3.2.1

[160] E. Hoogeboom, T. S. Cohen, and J. M. Tomczak, "Learning discrete distributions by dequantization," *arXiv preprint arXiv:2001.11235*, 2020. 3.1.3, 3.2.1

[161] T. Che, R. Zhang, J. Sohl-Dickstein, H. Larochelle, L. Paull, Y. Cao, and Y. Bengio, "Your gan is secretly an energy-based model and you should use discriminator driven latent sampling," in *Proceedings of the 34th International Conference on Neural Information Processing Systems*, ser. NIPS'20. Red Hook, NY, USA: Curran Associates Inc., 2020. 3.1.3

[162] G. Desjardins, Y. Bengio, and A. C. Courville, "On tracking the partition function," in *Advances in Neural Information Processing Systems*, J. Shawe-Taylor, R. Zemel, P. Bartlett, F. Pereira, and K. Weinberger, Eds., vol. 24. Curran Associates, Inc., 2011. [Online]. Available: <https://proceedings.neurips.cc/paper/2011/file/861dc9bd7f4e7dd3cccd534d0ae2a2e9-Paper.pdf> 3.1.3

[163] J. Lazarow, L. Jin, and Z. Tu, "Introspective neural networks for generative modeling," in *Proceedings of the IEEE International Conference on Computer Vision*, 2017, pp. 2774–2783. 3.1.3

[164] K. Lee, W. Xu, F. Fan, and Z. Tu, "Wasserstein introspective neural networks," in *Proceedings of the IEEE Conference on Computer Vision and Pattern Recognition*, 2018, pp. 3702–3711. 3.1.3

[165] L. Alili, P. Graczyk, and T. Zak, "On inversions and doob h-transforms of linear diffusions," *Lecture Notes in Mathematics*, vol. 2137, 09 2012. 3.1.4

[166] B. Uria, I. Murray, and H. Larochelle, "Rnade: The real-valued neural autoregressive density-estimator," *Advances in Neural Information Processing Systems*, vol. 26, 2013. 3.2.1

[167] F. Pomerleau, F. Colas, R. Siegwart *et al.*, "A review of point cloud registration algorithms for mobile robotics," *Foundations and Trends® in Robotics*, vol. 4, no. 1, pp. 1–104, 2015. 3.2.1

[168] A. Nguyen and B. Le, "3d point cloud segmentation: A survey," in *2013 6th IEEE conference on robotics, automation and mechatronics (RAM)*. IEEE, 2013, pp. 225–230. 3.2.1

[169] A. Vaswani, N. Shazeer, N. Parmar, J. Uszkoreit, L. Jones, A. N. Gomez, Ł. Kaiser, and I. Polosukhin, "Attention is all you need," *Advances in neural information processing systems*, vol. 30, 2017. 3.2.2

[170] J. Devlin, M.-W. Chang, K. Lee, and K. Toutanova, "Bert: Pre-training of deep bidirectional transformers for language understanding," *arXiv preprint arXiv:1810.04805*, 2018. 3.2.2

[171] A. Nichol, P. Dhariwal, A. Ramesh, P. Shyam, P. Mishkin, B. McGrew, I. Sutskever, and M. Chen, "Glide: Towards photorealistic image generation and editing with text-guided diffusion models," *arXiv preprint arXiv:2112.10741*, 2021. 3.2.2, 4.1.2, 3, 9

[172] A. Ramesh, P. Dhariwal, A. Nichol, C. Chu, and M. Chen, "Hierarchical text-conditional image generation with clip latents," *arXiv preprint arXiv:2204.06125*, 2022. 3.2.2

[173] J. Jumper, R. Evans, A. Pritzel, T. Green, M. Figurnov, O. Ronneberger, K. Tunyasuvunakool, R. Bates, A. Žídek, A. Potapenko *et al.*, "Highly accurate protein structure prediction with alphafold," *Nature*, vol. 596, no. 7873, pp. 583–589, 2021. 3.2.2

[174] S. Ovchinnikov and P.-S. Huang, "Structure-based protein design with deep learning," *Current opinion in chemical biology*, vol. 65, pp. 136–144, 2021. 3.2.2

[175] A. Van Den Oord, O. Vinyals *et al.*, "Neural discrete representation learning," *Advances in neural information processing systems*, vol. 30, 2017. 3.2.2, 3.3

[176] W. Fan, Y. Ma, Q. Li, Y. He, E. Zhao, J. Tang, and D. Yin, "Graph neural networks for social recommendation," in *The world wide web conference*, 2019, pp. 417–426. 3.2.3

[177] C. Huang, H. Xu, Y. Xu, P. Dai, L. Xia, M. Lu, L. Bo, H. Xing, X. Lai, and Y. Ye, "Knowledge-aware coupled graph neural network for social recommendation," in *Proceedings of the AAAI Conference on Artificial Intelligence*, vol. 35, no. 5, 2021, pp. 4115–4122. 3.2.3

[178] B. Jing, S. Eismann, P. Suriana, R. J. L. Townshend, and R. Dror, "Learning from protein structure with geometric vector perceptrons," in *International Conference on Learning Representations*, 2020. 3.2.3

[179] V. G. Satorras, E. Hoogeboom, and M. Welling, "E (n) equivariant graph neural networks," in *International conference on machine learning*. PMLR, 2021, pp. 9323–9332. 3.2.3

[180] H. Lin, Z. Gao, Y. Xu, L. Wu, L. Li, and S. Z. Li, "Conditional local convolution for spatio-temporal meteorological forecasting," in *Proceedings of the AAAI Conference on Artificial Intelligence*, vol. 36, no. 7, 2022, pp. 7470–7478. 3.2.3

[181] B. Yu, H. Yin, and Z. Zhu, "Spatio-temporal graph convolutional networks: A deep learning framework for traffic forecasting," *arXiv preprint arXiv:1709.04875*, 2017. 3.2.3

[182] H. A. Pierson and M. S. Gashler, "Deep learning in robotics: a review of recent research," *Advanced Robotics*, vol. 31, no. 16, pp. 821–835, 2017. 3.2.3

[183] R. P. De Lima, K. Marfurt, D. Duarte, and A. Bonar, "Progress and challenges in deep learning analysis of geoscience images," in *81st EAGE Conference and Exhibition 2019*, vol. 2019, no. 1. European Association of Geoscientists & Engineers, 2019, pp. 1–5. 3.2.3

[184] J. Wang, H. Cao, J. Z. Zhang, and Y. Qi, "Computational protein design with deep learning neural networks," *Scientific reports*, vol. 8, no. 1, pp. 1–9, 2018. 3.2.3

[185] W. Cao, Z. Yan, Z. He, and Z. He, "A comprehensive survey on geometric deep learning," *IEEE Access*, vol. 8, pp. 35 929–35 949, 2020. 3.2.3

[186] G. Wanner and E. Hairer, *Solving ordinary differential equations II*. Springer Berlin Heidelberg New York, 1996, vol. 375. 3.2.3

[187] L. Wu, H. Lin, Z. Gao, C. Tan, and S. Z. Li, "Self-supervised on graphs: Contrastive, generative, or predictive," 2021. 3.2.3

[188] I. Higgins, L. Matthey, A. Pal, C. Burgess, X. Glorot, M. Botvinick, S. Mohamed, and A. Lerchner, "beta-vae: Learning basic visual concepts with a constrained variational framework," 2016. 3.3

[189] F. Vargas, P. Thodoroff, A. Lamacraft, and N. Lawrence, "Solving schrödinger bridges via maximum likelihood," *Entropy*, vol. 23, no. 9, p. 1134, 2021. 3.3.1

[190] V. De Bortoli, J. Thornton, J. Heng, and A. Doucet, "Diffusion schrödinger bridge with applications to score-based generative modeling," *Advances in Neural Information Processing Systems*, vol. 34, pp. 17 695–17 709, 2021. 3.3.1

[191] C. Cremer, X. Li, and D. Duvenaud, "Inference suboptimality in variational autoencoders," in *International Conference on Machine Learning*. PMLR, 2018, pp. 1078–1086. 3.3.2

[192] B. Kawar, M. Elad, S. Ermon, and J. Song, "Denoising diffusion restoration models," in *ICLR Workshop on Deep Generative Models for Highly Structured Data*, 2022. 4.1.1, 3, 9

[193] L. Theis, T. Salimans, M. D. Hoffman, and F. Mentzer, "Lossy compression with gaussian diffusion," *arXiv preprint arXiv:2206.08889*, 2022. 4.1.1, 3, 9

[194] A. Lugmayr, M. Danelljan, A. Romero, F. Yu, R. Timofte, and L. Van Gool, "Repaint: Inpainting using denoising diffusion probabilistic models," in *Proceedings of the IEEE/CVF Conference on Computer Vision and Pattern Recognition*, 2022, pp. 11461–11471. 4.1.1, 3, 9

[195] A. Radford, J. W. Kim, C. Hallacy, A. Ramesh, G. Goh, S. Agarwal, G. Sastry, A. Askell, P. Mishkin, J. Clark *et al.*, "Learning transferable visual models from natural language supervision," in *International Conference on Machine Learning*. PMLR, 2021, pp. 8748–8763. 4.1.2, 6

[196] B. Poole, A. Jain, J. T. Barron, and B. Mildenhall, "Dreamfusion: Text-to-3d using 2d diffusion," *arXiv preprint arXiv:2209.14988*, 2022. 4.1.2, 3, 9

[197] T. Amit, E. Nachmani, T. Shaharbany, and L. Wolf, "Segdiff: Image segmentation with diffusion probabilistic models," *arXiv preprint arXiv:2112.00390*, 2021. 4.1.2, 3, 9

[198] J. Ho, T. Salimans, A. A. Gritsenko, W. Chan, M. Norouzi, and D. J. Fleet, "Video diffusion models," in *ICLR Workshop on Deep Generative Models for Highly Structured Data*, 2022. 4.1.2, 4.1.4, 3, 9

[199] A. Krizhevsky, I. Sutskever, and G. E. Hinton, "Imagenet classification with deep convolutional neural networks," *Communications of the ACM*, vol. 60, no. 6, pp. 84–90, 2017. C

[200] T.-Y. Lin, M. Maire, S. Belongie, J. Hays, P. Perona, D. Ramanan, P. Dollár, and C. L. Zitnick, "Microsoft coco: Common objects in context," in *European conference on computer vision*. Springer, 2014, pp. 740–755. 4.1.2

[201] P. Sanchez and S. A. Tsaftaris, "Diffusion causal models for counterfactual estimation," in *First Conference on Causal Learning and Reasoning*, 2021. 4.1.2

[202] L. Zhou, Y. Du, and J. Wu, "3d shape generation and completion through point-voxel diffusion," in *Proceedings of the IEEE/CVF International Conference on Computer Vision*, 2021, pp. 5826–5835. 4.1.3, 3, 9

[203] R. Yang, P. Srivastava, and S. Mandt, "Diffusion probabilistic modeling for video generation," *arXiv preprint arXiv:2203.09481*, 2022. 4.1.4, 3, 9

[204] W. Harvey, S. Naderiparizi, V. Masrani, C. Weilbach, and F. Wood, "Flexible diffusion modeling of long videos," *arXiv preprint arXiv:2205.11495*, 2022. 4.1.4, 3, 9

[205] Y. Song, L. Shen, L. Xing, and S. Ermon, "Solving inverse problems in medical imaging with score-based generative models," in *International Conference on Learning Representations*, 2021. 4.1.5, 3, 9

[206] H. Chung, E. S. Lee, and J. C. Ye, "Mr image denoising and super-resolution using regularized reverse diffusion," *arXiv preprint arXiv:2203.12621*, 2022. 4.1.5, 3, 9

[207] P. Sanchez, A. Kascenas, X. Liu, A. Q. O'Neil, and S. A. Tsaftaris, "What is healthy? generative counterfactual diffusion for lesion localization," *arXiv preprint arXiv:2207.12268*, 2022. 4.1.5

[208] S. W. Park, K. Lee, and J. Kwon, "Neural markov controlled sde: Stochastic optimization for continuous-time data," in *International Conference on Learning Representations*, 2021. 4.2.2, 3, 9

[209] M. Jeong, H. Kim, S. J. Cheon, B. J. Choi, and N. S. Kim, "Diff-TTS: A Denoising Diffusion Model for Text-to-Speech," in *Proc. Interspeech 2021*, 2021, pp. 3605–3609. 4.3, 3, 9

[210] V. Popov, I. Vovk, V. Gogoryan, T. Sadekova, M. S. Kudinov, and J. Wei, "Diffusion-based voice conversion with fast maximum likelihood sampling scheme," in *International Conference on Learning Representations*, 2021. 4.3, 3, 9

[211] D. Yang, J. Yu, H. Wang, W. Wang, C. Weng, Y. Zou, and D. Yu, "Diffsound: Discrete diffusion model for text-to-sound generation," *arXiv preprint arXiv:2207.09983*, 2022. 3, 4.3, 9

[212] S. Liu, Y. Cao, D. Su, and H. Meng, "Diffsvc: A diffusion probabilistic model for singing voice conversion," in *2021 IEEE Automatic Speech Recognition and Understanding Workshop (ASRU)*. IEEE, 2021, pp. 741–748. 3, 9

[213] A. Levkovitch, E. Nachmani, and L. Wolf, "Zero-shot voice conditioning for denoising diffusion tts models," *arXiv preprint arXiv:2206.02246*, 2022. 3, 4.3, 9

[214] Y. Leng, Z. Chen, J. Guo, H. Liu, J. Chen, X. Tan, D. Mandic, L. He, X.-Y. Li, T. Qin *et al.*, "Binauralgrad: A two-stage conditional diffusion probabilistic model for binaural audio synthesis," *arXiv preprint arXiv:2205.14807*, 2022. 3, 4.3, 9

[215] C. Shi, S. Luo, M. Xu, and J. Tang, "Learning gradient fields for molecular conformation generation," in *International Conference on Machine Learning*. PMLR, 2021, pp. 9558–9568. 3, 4.4.1, 9

[216] G. Corso, H. Stärk, B. Jing, R. Barzilay, and T. Jaakkola, "Diffdock: Diffusion steps, twists, and turns for molecular docking," *arXiv preprint arXiv:2210.01776*, 2022. 3, 4.4.1, 9

[217] T. Xie, X. Fu, O.-E. Ganea, R. Barzilay, and T. S. Jaakkola, "Crystal diffusion variational autoencoder for periodic material generation," in *International Conference on Learning Representations*, 2021. 3, 4.4.2, 9

[218] J. S. Lee and P. M. Kim, "Proteinsgm: Score-based generative modeling for de novo protein design," *bioRxiv*, 2022. 3, 4.4.2, 9

[219] K. E. Wu, K. K. Yang, R. v. d. Berg, J. Y. Zou, A. X. Lu, and A. P. Amini, "Protein structure generation via folding diffusion," *arXiv preprint arXiv:2209.15611*, 2022. 3, 4.4.2, 9

[220] Z. Chen, X. Tan, K. Wang, S. Pan, D. Mandic, L. He, and S. Zhao, "Infergrad: Improving diffusion models for vocoder by considering inference in training," in *ICASSP 2022-2022 IEEE International Conference on Acoustics, Speech and Signal Processing (ICASSP)*. IEEE, 2022, pp. 8432–8436. 4.3

[221] W. Jin, J. Wohlwend, R. Barzilay, and T. S. Jaakkola, "Iterative refinement graph neural network for antibody sequence-structure co-design," in *International Conference on Learning Representations*, 2021. 4.4.2

[222] T. Fu and J. Sun, "Antibody complementarity determining regions (cdrs) design using constrained energy model," in *Proceedings of the 28th ACM SIGKDD Conference on Knowledge Discovery and Data Mining*, 2022, pp. 389–399. 4.4.2

[223] W. Jin, R. Barzilay, and T. Jaakkola, "Antibody-antigen docking and design via hierarchical structure refinement," in *International Conference on Machine Learning*. PMLR, 2022, pp. 10217–10227. 4.4.2

[224] A. Borji, "Pros and cons of gan evaluation measures: New developments," *Computer Vision and Image Understanding*, vol. 215, p. 103329, 2022. B.1

[225] T. Salimans, I. Goodfellow, W. Zaremba, V. Cheung, A. Radford, and X. Chen, "Improved techniques for training gans," *Advances in neural information processing systems*, vol. 29, 2016. B.1

[226] S. Kullback, *Information theory and statistics*. Courier Corporation, 1997. B.1

[227] M. Heusel, H. Ramsauer, T. Unterthiner, B. Nessler, and S. Hochreiter, "Gans trained by a two time-scale update rule converge to a local nash equilibrium," in *Advances in Neural Information Processing Systems*, I. Guyon, U. V. Luxburg, S. Bengio, H. Wallach, R. Fergus, S. Vishwanathan, and R. Garnett, Eds., vol. 30. Curran Associates, Inc., 2017. [Online]. Available: <https://proceedings.neurips.cc/paper/2017/file/8a1d694707eb0fefe65871369074926d-Paper.pdf> B.2

[228] A. Razavi, A. Van den Oord, and O. Vinyals, "Generating diverse high-fidelity images with vq-vae-2," *Advances in neural information processing systems*, vol. 32, 2019. B.3

[229] T. M. Nguyen, A. Garg, R. G. Baraniuk, and A. Anandkumar, "Infocnf: Efficient conditional continuous normalizing flow using adaptive solvers," 2019. B.3

[230] Z. Ziegler and A. Rush, "Latent normalizing flows for discrete sequences," in *International Conference on Machine Learning*. PMLR, 2019, pp. 7673–7682. B.3

[231] J. Tomczak and M. Welling, "Vae with a vampprior," in *International Conference on Artificial Intelligence and Statistics*. PMLR, 2018, pp. 1214–1223. B.3

[232] O. Rybkin, K. Daniilidis, and S. Levine, "Simple and effective vae training with calibrated decoders," in *International Conference on Machine Learning*. PMLR, 2021, pp. 9179–9189. B.3

[233] A. Krizhevsky, G. Hinton *et al.*, "Learning multiple layers of features from tiny images," 2009. C

[234] Z. Liu, P. Luo, X. Wang, and X. Tang, "Deep learning face attributes in the wild," in *Proceedings of International Conference on Computer Vision (ICCV)*, December 2015. C

[235] F. Yu, A. Seff, Y. Zhang, S. Song, T. Funkhouser, and J. Xiao, "Lsun: Construction of a large-scale image dataset using deep learning with humans in the loop," *arXiv preprint arXiv:1506.03365*, 2015. C

[236] T. Karras, S. Laine, and T. Aila, "A style-based generator architecture for generative adversarial networks," in *Proceedings of the IEEE/CVF Conference on Computer Vision and Pattern Recognition (CVPR)*, June 2019. C

- [237] Y. LeCun and C. Cortes, "MNIST handwritten digit database," 2010. [Online]. Available: <http://yann.lecun.com/exdb/mnist/>
- [238] H. Chung, B. Sim, D. Ryu, and J. C. Ye, "Improving diffusion models for inverse problems using manifold constraints," *arXiv preprint arXiv:2206.00941*, 2022. 5
- [239] Y. Song and S. Ermon, "Improved techniques for training score-based generative models," *Advances in neural information processing systems*, vol. 33, pp. 12 438–12 448, 2020. 6, 8

APPENDIX A

SAMPLING ALGORITHMS

Algorithm 1 Ancestral Sampling

```

 $x_T \sim \mathcal{N}(0, I)$ 
for  $t = T, \dots, 1$  do
  if  $t > 1$  then
     $z \sim \mathcal{N}(0, I)$ 
  else
     $F = 0$ 
  end if
   $x_{t-1} = \frac{1}{\sqrt{\alpha_t}} \left( x_t - \frac{1-\alpha_t}{\sqrt{1-\alpha_t}} \epsilon_\theta(x_t, t) \right) + \sigma_t z$ 
end for
return  $x_0$ 

```

Algorithm 2 Annealed Langevin Dynamics Sampling

```

Initialize  $x_0$ 
for  $i = 1, \dots, L$  do
   $\alpha_i \leftarrow \epsilon \cdot \sigma_i^2 / \sigma_L^2$ 
  for  $t = 1, \dots, L$  do
     $z_t \sim \mathcal{N}(0, I)$ 
     $\tilde{x}_t = \tilde{x}_{t-1} + \frac{\alpha_i}{2} s_\theta(\tilde{x}_{t-1}, \sigma_i) + \sqrt{\alpha_i} z_t$ 
  end for
   $\tilde{x}_0 \leftarrow \tilde{x}_T$ 
end for
return  $\tilde{x}_T$ 

```

Algorithm 3 Predictor-Corrector Sampling(VE SDE)

```

 $x_N \sim \mathcal{N}(0, \sigma_{\max}^2 I)$ 
for  $i = N - 1$  to 0 do
   $x'_i \leftarrow x_{i+1} + (\sigma_{i+1}^2 - \sigma_i^2) s_\theta * (x_{i+1}, \sigma_{i+1})$ 
   $Z \sim \mathcal{N}(0, I)$ 
   $x_i \leftarrow x'_i + \sqrt{\sigma_{i+1}^2 - \sigma_i^2} z$ 
  for  $j = 1$  to  $M$  do
     $Z \sim \mathcal{N}(0, I)$ 
     $x_i \leftarrow x_i + \epsilon_i s_\theta * (x_i, \sigma_i) + \sqrt{2\epsilon_i} z$ 
  end for
end for
return  $x_0$ 

```

Algorithm 4 Predictor-Corrector Sampling(VP SDE)

```

 $x_N \sim \mathcal{N}(0, I)$ 
for  $i = N - 1$  to 0 do
   $x'_i \leftarrow \left( 2 - \sqrt{1 - \beta_{i+1}} \right) x_{i+1} + \beta_{i+1} s_\theta * (x_{i+1}, i + 1)$ 
   $Z \sim \mathcal{N}(0, I)$ 
   $x_i \leftarrow x'_i + \sqrt{\beta_{i+1}} z$ 
  for  $j = 1$  to  $M$  do
     $Z \sim \mathcal{N}(0, I)$ 
     $x_i \leftarrow x_i + \epsilon_i s_\theta * (x_i, \sigma_i) + \sqrt{2\epsilon_i} z$ 
  end for
end for
return  $x_0$ 

```

Algorithm 5 Cold Diffusion Sampling

```

Input: A degraded sample  $x_t$ 
for  $s = t, t - 1, \dots, 1$  do
   $\hat{x}_0 \leftarrow R(x_s, s)$ 
   $x_{s-1} = x_s - D(\hat{x}_0, s) + D(\hat{x}_0, s - 1)$ 
end for
return  $x_0$ 

```

APPENDIX B

EVALUATION METRIC

To evaluate the properties of generated samples, Evaluation metrics are designed to test the sample quality and diversity.

B.1 Inception Score (IS)

The inception score is built to value the diversity and resolution of generated images based on the ImageNet dataset [224], [225]. It can be divided into two parts: diversity measurement and quality measurement. Diversity measurement denoted by p_{IS} is calculated w.r.t. the class entropy of generated samples: the larger the entropy is, the more diverse the samples will be. Quality measurement denoted by q_{IS} is computed through the similarity between a sample and the related class images using entropy. It is because the samples will enjoy high resolution if they are closer to the specific class of images in the ImageNet dataset. Thus, to lower q_{IS} and higher p_{IS} , the KL divergence [226] is applied to inception score calculation:

$$\begin{aligned}
 IS &= D_{KL}(p_{IS} \parallel q_{IS}) \\
 &= \mathbb{E}_{x \sim p_{IS}} \left[\log \frac{p_{IS}}{q_{IS}} \right] \\
 &= \mathbb{E}_{x \sim p_{IS}} [\log(p_{IS}) - \log(q_{IS})]
 \end{aligned} \tag{40}$$

B.2 Frechet Inception Distance (FID)

Although there are reasonable evaluation techniques in the Inception Score, the establishment is based on a specific dataset with 1000 classes and a trained network that consists of randomness such as initial weights, and code framework. Thus, the bias between ImageNet and real-world images may cause an inaccurate outcome. Furthermore, the number of sample batches is much less than 1000 classes, leading to a value

FID is proposed to solve the bias from the specific reference datasets. The score shows the distance between real-world data distribution and the generated samples using the mean and the covariance [227].

$$FID = \|\mu_r - \mu_g\|^2 + \text{Tr} \left(\Sigma_r + \Sigma_g - 2 (\Sigma_r \Sigma_g)^{1/2} \right) \tag{41}$$

where μ_g, Σ_g are the mean and covariance of generated samples, and μ_r, Σ_r are the mean and covariance of real-world data.

B.3 Negative Log Likelihood (NLL)

According to Razavi *et al.*, [228] negative log-likelihood is seen as a common evaluation metric that describes all modes of data distribution. Lots of works on normalizing flow field [229], [230] and VAE field [231], [232] uses NLL as one of the choices for evaluation. Some diffusion models like improved DDPM [60] regard the NLL as the training objective.

$$\text{NLL} = \mathbb{E} [-\log p_\theta(x)] \quad (42)$$

APPENDIX C BENCHMARKS

The benchmarks of landmark models along with improved techniques corresponding to **FID score**, **Inception Score**, and **NLL** are provided on diverse datasets which includes CIFAR-10 [233], ImageNet [199], and CelebA-64 [234]. In addition, some dataset-based performances such as LSUN [235], FFHQ [236], and MNIST [237] are not presented since there is much less experiment data. The selected performance are listed according to NFE in descending order to compare for easier access.

C.1 Benchmarks on CelebA-64

TABLE 4
Benchmarks on CelebA-64

Method	NFE	FID	NLL
NPR-DDIM [92]	1000	3.15	-
SN-DDIM [92]	1000	2.90	-
NCSN [69]	1000	10.23	-
NCSN ++ [123]	1000	1.92	1.97
DDPM ++ [123]	1000	1.90	2.10
DiffuseVAE [99]	1000	4.76	-
Analytic DPM [91]	1000	-	2.66
ES-DDPM [86]	200	2.55	-
PNDM [76]	200	2.71	-
ES-DDPM [86]	100	3.01	-
PNDM [76]	100	2.81	-
Analytic DPM [91]	100	-	2.66
NPR-DDIM [92]	100	4.27	-
SN-DDIM [92]	100	3.04	-
ES-DDPM [86]	50	3.97	-
PNDM [76]	50	3.34	-
NPR-DDIM [92]	50	6.04	-
SN-DDIM [92]	50	3.83	-
DPM-Solver Discrete [63]	36	2.71	-
ES-DDPM [86]	20	4.90	-
PNDM [76]	20	5.51	-
DPM-Solver Discrete [63]	20	2.82	-
ES-DDPM [86]	10	6.44	-
PNDM [76]	10	7.71	-
Analytic DPM [91]	10	-	2.97
NPR-DDPM [92]	10	28.37	-
SN-DDPM [92]	10	20.60	-
NPR-DDIM [92]	10	14.98	-
SN-DDIM [92]	10	10.20	-
DPM-Solver Discrete [63]	10	6.92	-
ES-DDPM [86]	5	9.15	-
PNDM [76]	5	11.30	-

C.2 Benchmarks on ImageNet-64

TABLE 5
Benchmarks on ImageNet-64

Method	NFE	FID	IS	NLL
MCG [238]	1000	25.4	-	-
Analytic DPM [91]	1000	-	-	3.61
ES-DDPM [86]	900	2.07	55.29	-
Efficient Sampling [95]	256	3.87	-	-
Analytic DPM [91]	200	-	-	3.64
NPR-DDPM [92]	200	16.96	-	-
SN-DDPM [92]	200	16.61	-	-
ES-DDPM [86]	100	3.75	48.63	-
DPM-Solver Discrete [63]	57	17.47	-	-
ES-DDPM [86]	25	3.75	48.63	-
GGDM [98]	25	18.4	18.12	-
Analytic DPM [91]	25	-	-	3.83
NPR-DDPM [92]	25	28.27	-	-
SN-DDPM [92]	25	27.58	-	-
DPM-Solver Discrete [63]	20	18.53	-	-
ES-DDPM [86]	10	3.93	48.81	-
GGDM [98]	10	37.32	14.76	-
DPM-Solver Discrete [63]	10	24.4	-	-
ES-DDPM [86]	5	4.25	48.04	-
GGDM [98]	5	55.14	12.9	-

C.3 Benchmarks on CIFAR-10 Dataset

TABLE 6
Benchmarks on CIFAR-10 (NFE ≥ 1000)

Method	NFE	FID	IS	NLL
Improved DDPM [60]	4000	2.90	-	-
VE SDE [65]	2000	2.20	9.89	-
VP SDE [65]	2000	2.41	9.68	3.13
sub-VP SDE [65]	2000	2.41	9.57	2.92
DDPM [67]	1000	3.17	9.46	3.72
NCSN [69]	1000	25.32	8.87	-
SSM [77]	1000	54.33	-	-
NCSNv2 [239]	1000	10.87	8.40	-
D3PM [64]	1000	7.34	8.56	3.44
Efficient Sampling [97]	1000	2.94	-	-
NCSN++ [123]	1000	2.33	10.11	3.04
DDPM++ [123]	1000	2.47	9.78	2.91
TDPM [85]	1000	3.07	9.24	-
VDM [66]	1000	4.00	-	-
DiffuseVAE [99]	1000	8.72	8.63	-
Analytic DPM [91]	1000	-	-	3.59
NPR-DDPM [92]	1000	4.27	-	-
SN-DDPM [92]	1000	4.07	-	-
Gotta Go Fast VP [93]	1000	2.49	-	-
Gotta Go Fast VE [93]	1000	3.14	-	-
INDM [104]	1000	2.28	-	3.09

TABLE 7
Benchmarks on CIFAR-10 (NFE < 1000)

Method	NFE	FID	IS	NLL
Diffusion Step [88]	600	3.72	-	-
ES-DDPM [86]	600	3.17	-	-
Diffusion Step [88]	400	14.38	-	-
Diffusion Step [88]	200	5.44	-	-
NPR-DDPM [92]	200	4.10	-	-
SN-DDPM [92]	200	3.72	-	-
Gotta Go Fast VP [93]	180	2.44	-	-
Gotta Go Fast VE [93]	180	3.40	-	-
LSGM [101]	138	2.10	-	-
DDIM [68]	100	4.16	-	-
FastDPM [89]	100	2.86	-	-
TDPM [85]	100	3.10	9.34	-
NPR-DDPM [92]	100	4.52	-	-
SN-DDPM [92]	100	3.83	-	-
DiffuseVAE [99]	100	11.71	8.27	-
DiffFlow [100]	100	14.14	-	3.04
Analytic DPM [91]	100	-	-	3.59
Efficient Sampling [97]	64	3.08	-	-
DPM-Solver [63]	51	2.59	-	-
DDIM [68]	50	4.67	-	-
FastDPM [89]	50	3.2	-	-
NPR-DDPM [92]	50	5.31	-	-
SN-DDPM [92]	50	4.17	-	-
Improved DDPDM [60]	50	4.99	-	-
TDPM [85]	50	3.3	9.22	-
DEIS [97]	50	2.57	-	-
gDDIM [94]	50	2.28	-	-
DPM-Solver Discrete [63]	44	3.48	-	-
iODE [96]	35	1.79	-	-
Efficient Sampling [97]	32	3.17	-	-
Improved DDPDM [60]	25	7.53	-	-
GGDM [98]	25	4.25	9.19	-
NPR-DDPM [92]	25	7.99	-	-
SN-DDPM [92]	25	6.05	-	-
DDIM [68]	20	6.84	-	-
FastDPM [89]	20	5.05	-	-
DEIS [97]	20	2.86	-	-
DPM-Solver [63]	20	2.87	-	-
DPM-Solver Discrete [63]	20	3.72	-	-
Efficient Sampling [97]	16	3.41	-	-
NPR-DDPM [92]	10	19.94	-	-
SN-DDPM [92]	10	16.33	-	-
DDIM [68]	10	13.36	-	-
FastDPM [89]	10	9.90	-	-
GGDM [98]	10	8.23	8.90	-
Analytic DPM [91]	10	-	-	4.11
DEIS [97]	10	4.17	-	-
DPM-Solver [63]	10	6.96	-	-
DPM-Solver Discrete [63]	10	10.16	-	-
Progressive Distillation [61]	8	2.57	-	-
Denoising Diffusion GAN [62]	8	4.36	9.43	-
GGDM [98]	5	13.77	8.53	-
DEIS [97]	5	15.37	-	-
Progressive Distillation [61]	4	3.00	-	-
TDPM [85]	4	3.41	9.00	-
Denoising Diffusion GAN [62]	4	3.75	9.63	-
Progressive Distillation [61]	2	4.51	-	-
TDPM [85]	2	4.47	8.97	-
Denoising Diffusion GAN [62]	2	4.08	9.80	-
Denoising student [84]	1	9.36	8.36	-
Progressive Distillation [61]	1	9.12	-	-
TDPM [85]	1	8.91	8.65	-

TABLE 8
Details for Improved Diffusion Methods

Method	Year	Data	Model	Framework	Training	Sampling	Code
Landmark Works							
DPM [25]	2015	RGB Image	Discrete	Diffusion	L_{simple}	Ancestral	[code]
DDPM [67]	2020	RGB Image	Discrete	Diffusion	L_{simple}	Ancestral	[code]
NCSN [69]	2019	RGB Image	Discrete	Score	L_{DSM}	Langevin dynamics	[code]
NCSNv2 [239]	2020	RGB Image	Discrete	Score	L_{DSM}	Langevin dynamics	[code]
Score SDE [65]	2020	RGB Image	Continuous	SDE	L_{DSM}	PC-Sampling	[code]
Improved Works							
Progressive Distill [61]	2022	RGB Image	Discrete	Diffusion	L_{simple}	DDIM Sampling	[code]
Denoising Student [84]	2021	RGB Image	Discrete	Diffusion	$L_{Distill}$	DDIM Sampling	[code]
TDPM [85]	2022	RGB Image	Discrete	Diffusion	$L_{DDPM\&GAN}$	Ancestral	-
ES-DDPM [86]	2022	RGB Image	Discrete	Diffusion	$L_{DDPM\&VAE}$	Conditional Sampling	[code]
CCDF [87]	2021	RGB Image	Discrete	SDE	L_{simple}	Langevin dynamics	[code]
Franzese's Model [88]	2022	RGB Image	Continuous	SDE	L_{DSM}	DDIM Sampling	-
FastDPM [89]	2021	RGB Image	Discrete	Diffusion	L_{simple}	DDIM Sampling	[code]
Improved DDPM [60]	2021	RGB Image	Discrete	Diffusion	L_{hybrid}	Ancestral	[code]
VDM [66]	2022	RGB Image	Both	Diffusion	L_{simple}	Ancestral	[code]
San-Roman's Model [90]	2021	RGB Image	Discrete	Diffusion	$L_{DDPM\&Noise}$	Ancestral	-
Analytic-DPM [91]	2022	RGB Image	Discrete	Score	$L_{Trajectory}$	Ancestral	[code]
NPR-DDPM [92]	2022	RGB Image	Discrete	Diffusion	$L_{DDPM\&Noise}$	Ancestral	[code]
SN-DDPM [92]	2022	RGB Image	Discrete	Score	L_{square}	Ancestral	[code]
DDIM [68]	2021	RGB Image	Discrete	Diffusion	L_{simple}	DDIM Sampling	[code]
gDDIM [94]	2022	RGB Image	Continuous	SDE&ODE	L_{DSM}	PC-Sampling	[code]
INDM [104]	2022	RGB Image	Continuous	SDE	$L_{DDPM\&Flow}$	PC-Sampling	-
Ito-Taylor [23]	2021	RGB Image	Continuous	SDE	L_{DSM}	Ideal Derivatives Sampling	-
Gotta Go Fast [93]	2021	RGB Image	Continuous	SDE	L_{DSM}	Improved Euler	[code]
DPM-Solver [63]	2022	RGB Image	Continuous	ODE	L_{DSM}	Higher ODE solvers	[code]
iODE [96]	2022	RGB Image	Continuous	ODE	L_{DSM}	2 nd Order Heun	[code]
PNND [76]	2022	Manifold	Discrete	ODE	L_{simple}	Multi-step & Runge-Kutta	[code]
DDSS [98]	2021	RGB Image	Discrete	Diffusion	L_{simple}	Dynamic Programming	-
GGDM [95]	2022	RGB Image	Discrete	Diffusion	L_{KID}	Dynamic Programming	-
Diffusion GAN [62]	2022	RGB Image	Discrete	Diffusion	$L_{DDPM\&GAN}$	Ancestral	[code]
DiffuseVAE [99]	2022	RGB Image	Discrete	Diffusion	$L_{DDPM\&VAE}$	Ancestral	[code]
Diffusion Flow [100]	2021	RGB Image	Discrete	SDE	L_{DSM}	Langevin & Flow Sampling	[code]
LSGM [101]	2021	RGB Image	Continuous	ODE	$L_{DDPM\&VAE}$	ODE-Solver	[code]
Score-flow [102]	2021	Dequantization	Continuous	SDE	L_{DSM}	PC-Sampling	[code]
PDM [103]	2022	RGB Image	Continuous	SDE	L_{Gap}	PC-Sampling	-
Score-EBM [105]	2021	RGB Image	Discrete	Score	$L_{Recovery}$	Langevin dynamics	[code]
Song's Model [106]	2021	RGB Image	Discrete	Score	L_{DSM}	Langevin dynamics	-
Huang's Model [110]	2021	RGB Image	Continuous	SDE	L_{DSM}	SDE-Solver	[code]
De Bortoli's Model [109]	2021	RGB Image	Continuous	SDE	L_{DSM}	Importance Sampling	[code]
PVD [111]	2021	Point Cloud	Discrete	Diffusion	L_{simple}	Ancestral	[code]
Luo's Model [32]	2021	Point Cloud	Discrete	Diffusion	L_{simple}	Ancestral	[code]
Lyu's Model [33]	2022	Point Cloud	Discrete	Diffusion	L_{simple}	Farthest Point Sampling	[code]
D3PM [64]	2021	Categorical Data	Discrete	Diffusion	L_{hybrid}	Ancestral	[code]
Argmax [113]	2021	Categorical Data	Discrete	Diffusion	$L_{DDPM\&Flow}$	Gumbel sampling	[code]
ARDM [114]	2022	Categorical Data	Discrete	Diffusion	L_{simple}	Ancestral	[code]
Campbell's Model [115]	2022	Categorical Data	Continuous	Diffusion	L_{simple}^{CT}	PC-Sampling	[code]
VQ-diffusion [116]	2022	Vector-Quantized	Discrete	Diffusion	L_{simple}	Ancestral	[code]
Improved VQ-Diff [117]	2022	Vector-Quantized	Discrete	Diffusion	L_{simple}	Purity Prior Sampling	[code]
Cohen's Model [118]	2022	Vector-Quantized	Discrete	Diffusion	L_{simple}	Ancestral & VAE Sampling	[code]
Xie's Model [119]	2022	Vector-Quantized	Discrete	Diffusion	$L_{DDPM\&Class}$	Ancestral & VAE Sampling	-
RGSM [120]	2022	Manifold	Continuous	SDE	L_{DSM}	Geodesic Random Walk	-
RDM [121]	2022	Manifold	Continuous	SDE	L_{DSM}^{CT}	Importance Sampling	-
EDP-GNN [122]	2020	Graph	Discrete	Score	L_{DSM}	Langevin dynamics	[code]
NCSN++ [123]	2021	RGB Image	Continuous	SDE	L_{DSM}	PC-Sampling	[code]

TABLE 9
Details for Diffusion Applications

Method	Year	Data	Framework	Downstream Task	Code
Computer Vision					
CMDE [26]	2021	RGB-Image	SDE	Inpainting, Super-Resolution, Edge to image translation	[code]
DDRM [192]	2022	RGB-Image	Diffusion	Super-Resolution, Deblurring, Inpainting, Colorization	[code]
Palette [83]	2022	RGB-Image	Diffusion	Colorization, Inpainting, Uncropping, JPEG Restoration	[code]
DiffC [193]	2022	RGB-Image	SDE	Compression	-
SRDiff [28]	2021	RGB-Image	Diffusion	Super-Resolution -	
RePaint [194]	2022	RGB-Image	Diffusion	Inpainting, Super-resolution, Edge to Image Translation	[code]
FSDM [29]	2022	RGB-Image	Diffusion	Few-shot Generation	-
CARD [30]	2022	RGB-Image	Diffusion	Conditional Generation	[code]
GLIDE [171]	2022	RGB-Image	Diffusion	Conditional Generation	[code]
LSGM [101]	2022	RGB-Image	SDE	UnConditional & Conditional Generation	[code]
SegDiff [197]	2022	RGB-Image	Diffusion	Segmentation	-
VQ-Diffusion [116]	2022	VQ Data	Diffusion	Text-to-Image Synthesis	[code]
DreamFusion [196]	2023	VQ Data	Diffusion	Text-to-Image Synthesis	[code]
Text-to-Sign VQ [119]	2022	VQ Data	Diffusion	Conditional Pose Generation	-
Improved VQ-Diff [117]	2022	VQ Data	Diffusion	Text-to-Image Synthesis	-
Luo's Model [32]	2021	Point Cloud	Diffusion	Point Cloud Generation	[code]
PVD [202]	2022	Point Cloud	Diffusion	Point Cloud Generation, Point-Voxel representation	[code]
PDR [33]	2022	Point Cloud	Diffusion	Point Cloud Completion	[code]
Cheng's Model [112]	2022	Point Cloud	Diffusion	Point Cloud Generation	[code]
Luo's Model [34]	2022	Point Cloud	Score	Point Cloud Denoising	[code]
VDM [198]	2022	Video	Diffusion	Text-Conditioned Video Generation	[code]
RVD [203]	2022	Video	Diffusion	Video Forecasting, Video compression	[code]
FDM [204]	2022	Video	Diffusion	Video Forecasting, Long-range Video modeling	-
MCVD [35]	2022	Video	Diffusion	Video Prediction, Video Generation, Video Interpolation	[code]
RaMViD [36]	2022	Video	SDE	Conditional Generation	-
Score-MRI [37]	2022	MRI	SDE	MRI Reconstruction	[code]
Song's Model [205]	2022	MRI, CT	SDE	MRI Reconstruction, CT Reconstruction	[code]
R2D2+ [206]	2022	MRI	SDE	MRI Denoising	-
Sequence Modeling					
Diffusion-LM [38]	2022	Text	Diffusion	Conditional Text Generation	[code]
Bit Diffusion [39]	2022	Text	Diffusion	Image-Conditional Text Generation	[code]
D3PM [64]	2021	Text	Diffusion	Text Generation	-
Argmax [113]	2021	Text	Diffusion	Text Segmentation, Text Generation	[code]
CSDI [40]	2021	Time Series	Diffusion	Series Imputation	[code]
SSSD [41]	2022	Time Series	Diffusion	Series Imputation	[code]
CSDE [208]	2022	Time Series	SDE	Series Imputation, Series Prediction	-
Audio & Speech					
WaveGrad [42]	2020	Audio	Diffusion	Conditional Wave Generation	[code]
DiffWave [43]	2021	Audio	Diffusion	Conditional & Unconditional Wave Generation	[code]
GradTTS [44]	2021	Audio	SDE	Wave Generation	[code]
Diff-TTS [209]	2021	Audio	Diffusion	non-AR mel-Spectrogram Generation, Speech Synthesis	-
DiffVC [210]	2022	Audio	SDE	Voice conversion	[code]
DiffSVC [212]	2022	Audio	Diffusion	Voice Conversion	[code]
DiffSinger [45]	2022	Audio	Diffusion	Singing Voice Synthesis	[code]
Diffsound [211]	2021	Audio	Diffusion	Text-to-sound Generation tasks	[code]
EdiTTS [46]	2022	Audio	SDE	fine-grained pitch, content editing	[code]
Guided-TTS [47]	2022	Audio	SDE	Conditional Speech Generation	-
Guided-TTS2 [48]	2022	Audio	SDE	Conditional Speech Generation	-
Levkovitch's Model [213]	2022	Audio	SDE	Spectrograms-Voice Generation	[code]
SpecGrad [49]	2022	Audio	Diffusion	Spectrograms-Voice Generation	[code]
ItoTTS [24]	2022	Audio	SDE	Spectrograms-Voice Generation	-
ProDiff [31]	2022	Audio	Diffusion	Text-to-Speech Synthesis	[code]
BinauralGrad [214]	2022	Audio	Diffusion	Binaural Audio Synthesis	-
AI For Science					
ConfGF [215]	2021	Molecular	Score	Conformation Generation	[code]
DGSM [52]	2022	Molecular	Score	Conformation Generation, Sidechain Generation	-
GeoDiff [53]	2022	Molecular	Diffusion	Conformation Generation	[code]
EDM [21]	2022	Molecular	SDE	Conformation Generation	[code]
Torsional Diff [54]	2022	Molecular	Diffusion	Molecular Generation	[code]
DiffDock [216]	2022	Molecular&protein	Diffusion	Conformation Generation, molecular docking	[code]
CDVAE [217]	2022	Protein	Score	Periodic Material Generation	[code]
Luo's Model [55]	2022	Protein	Diffusion	CDR Generation	-
Anand's Model [56]	2022	Protein	Diffusion	Protein Sequence and Structure Generation	-
ProteinSGM [218]	2022	Protein	SDE	de novo protein design	-
DiffFolding [219]	2022	Protein	Diffusion	Protein Inverse Folding	[code]